NASA TECHNICAL MEMORANDUM

NASA TM X-1542

NASA TM X-1542

GPO PRICE $ _____

CFSTI PRICE(S) $ _____

Hard copy (HC) 3.00

Microfiche (MF) .65

ff 653 July 65

FACILITY FORM 602

N68-21778 (ACCESSION NUMBER)

53 (PAGES)

TMX 1542 (NASA CR OR TMX OR AD NUMBER)

1 (THRU)

(CODE)

31 (CATEGORY)

FLIGHT TEST OF A 30-FOOT-NOMINAL-DIAMETER CROSS PARACHUTE DEPLOYED AT A MACH NUMBER OF 1.57 AND A DYNAMIC PRESSURE OF 9.7 POUNDS PER SQUARE FOOT

by John S. Preisser and Clinton V. Eckstrom

Langley Research Center
Langley Station, Hampton, Va.

NATIONAL AERONAUTICS AND SPACE ADMINISTRATION • WASHINGTON, D. C. • APRIL 1968

NASA TM X-1542

FLIGHT TEST OF A 30-FOOT-NOMINAL-DIAMETER CROSS PARACHUTE DEPLOYED AT A MACH NUMBER OF 1.57 AND A DYNAMIC PRESSURE OF 9.7 POUNDS PER SQUARE FOOT

By John S. Preisser and Clinton V. Eckstrom

Langley Research Center
Langley Station, Hampton, Va.

Technical Film Supplement L-994 available on request.

NATIONAL AERONAUTICS AND SPACE ADMINISTRATION

For sale by the Clearinghouse for Federal Scientific and Technical Information
Springfield, Virginia 22151 – CFSTI price $3.00

FLIGHT TEST OF A 30-FOOT-NOMINAL-DIAMETER CROSS PARACHUTE DEPLOYED AT A MACH NUMBER OF 1.57 AND A DYNAMIC PRESSURE OF 9.7 POUNDS PER SQUARE FOOT

By John S. Preisser and Clinton V. Eckstrom
Langley Research Center

SUMMARY

A 30-foot (9.1-meter) nominal-diameter cross-type parachute with a cloth area (reference area) of 709 square feet (65.9 square meters) was flight tested in the rocket-launched portion of the NASA Planetary Entry Parachute Program (PEPP). The test parachute was ejected from an instrumented payload by means of a mortar when the system was at a Mach number of 1.57 and a dynamic pressure of 9.7 psf (460 N/m^2). The parachute deployed to suspension-line stretch in 0.44 second with a resulting snatch-force loading of 1100 pounds (4900 newtons). Canopy inflation began at 0.58 second and a first full inflation was achieved at approximately 0.77 second. The maximum opening load occurred at 0.81 second and was 4255 pounds (18 930 newtons). Thereafter, the test item exhibited a canopy-shape instability in that the four panel arms experienced fluctuations, a "scissoring" type of motion predominating throughout the test period. Calculated values of axial-force coefficient during the deceleration portion of the test varied between 0.35 and 1.05, with an average value of 0.69. During descent, canopy-shape variations had reduced to small amplitudes and resultant pitch-yaw angles of the payload with respect to the local vertical averaged less than 10°. The effective drag coefficient, based on the vertical components of velocity and acceleration during system descent, was 0.78. An earlier test of a 25.2-foot (7.7-meter) nominal-diameter cross parachute is described in appendix A, along with a brief analysis of the riser-line failure suffered during the test. Appendix B presents pertinent notes relating to an operational procedure involving an attitude reference system used in PEPP testing and the subsequent reduction of attitude data required by using this procedure.

INTRODUCTION

Parachutes have been used for many applications through the years; however, requirements for operation in low-density environments have been rather recent. Systems design for soft landing instrumented capsules on Mars, for example, require data on performance characteristics of decelerators which deploy at supersonic velocities in

a low-density atmosphere. At the present time, very little information is available for such operating conditions. The NASA Planetary Entry Parachute Program (PEPP) test series was established to provide desired flight data employing various parachute configurations with promising characteristics. (See ref. 1.) The principal results presented herein are from a PEPP test of a 30-foot (9.1-meter) nominal-diameter cross parachute having a reference area or cloth area of 709 square feet (65.9 square meters) and composed of two panels, each with a width-length ratio of 0.264. In addition, results are given from an earlier test of a 25.2-foot (7.7-meter) nominal-diameter cross parachute with 500 square feet (46 square meters) of cloth area and a 0.333 panel width-length ratio. A description of this earlier test parachute and a brief discussion of the riser line failure suffered during the test are presented in appendix A. Other PEPP results published to date include those from 85.3-, 31.2-, and 40-foot (26.0-, 9.5-, 12.2-meter) nominal-diameter modified ringsail parachutes and a 30-foot (9.1-meter) nominal-diameter disk-gap-band parachute, and are given in references 2 to 5.

The flight plan for these tests was aimed at deploying the test parachute at a Mach number of 1.60 and a dynamic pressure of 10 psf (479 N/m^2). Test objectives were to observe the characteristics of the parachute deployment and inflation, and to measure opening shock loads, parachute drag efficiency, and stability characteristics.

A motion-picture film supplement, taken by an onboard camera, shows deployment, inflation, and overall flight performance during the test of the 0.264 width-length ratio parachute.

SYMBOLS

$C_{A,o}$	axial-force coefficient
$\left(C_{D,o}\right)_{eff}$	effective drag coefficient (based on vertical descent velocity and acceleration)
D_o	nominal diameter, $\left(\frac{4}{\pi} S_o\right)^{1/2}$, feet (meters)
g	acceleration due to gravity, feet/second^2 (meters/second^2)
H,J,K,L	transformation matrices (defined in appendix B)
h_{ij}, j_{ij} k_{ij}, l_{ij}	elements of matrices H,J,K,L, respectively (i,j = 1,2,3)
M	Mach number

m	mass, slugs (kilograms)
q_∞	free-stream dynamic pressure, $\frac{1}{2}\rho_\infty V^2$, pounds/feet^2 (newtons/meter^2)
S_o	nominal or reference area of parachute canopy, feet^2 (meters^2) (see text for definition of use with cross design)
T	tensiometer force, pounds (newtons)
t	time from launch vehicle lift-off, seconds
t'	time from mortar firing, seconds
V	true airspeed, feet/second (meters/second)
X,Y,Z	payload body-axis system
X_f,Y_f,Z_f	earth-fixed axis system (refer to sketch in appendix B)
X_l,Y_l,Z_l	payload body-axis system at time of launch vehicle lift-off
X_o,Y_o,Z_o	inertial coordinate system corresponding to that position where the gyro platform would read "zero" in pitch, yaw, and roll
Z_E	local vertical axis
Λ	launch azimuth
Γ	-(launch elevation + 90^o)
δ_E	payload resultant pitch-yaw angle from local vertical, degrees
$\theta_g,\psi_g,\varphi_g$	gyro platform angles defining body-axis system relative to inertial coordinate system, degrees
$\theta_o,\psi_o,\varphi_o$	gyro platform angle readings at time of launch vehicle lift-off, degrees

$\theta_E, \psi_E, \varphi_E$ Euler angles relating body-axis system to earth-fixed axis system (refer to sketch in appendix B), degrees

ρ_∞ free-stream atmospheric density, slugs/feet^3 (kilograms/meters^3)

Dots over symbols denote differentiation with respect to time. Bars over symbols denote mean values averaged on a cycle-to-cycle basis.

TEST SYSTEM DESCRIPTION

The test payload was carried to the parachute deployment point by means of an Honest John – Nike rocket vehicle. A photograph of the vehicle configuration is presented in figure 1. A brief discussion of the launch vehicle system has been presented in reference 3; however, important aspects of that discussion are restated in this report. A radio command system was used to start a programer which, in turn, initiated the firing of the parachute deployment mortar. A real-time visual display of the variation of payload altitude with velocity which included grids of constant Mach number and constant dynamic pressure, such as is described in references 1 and 3, was used by the flight controller for guidance in determining the correct time for transmitting the radio command signal.

A diagram of the test payload is presented in figure 2. The payload weight including the parachute system for this test was 240 pounds (109 kilograms). Onboard instrumentation consisted of a tensiometer placed in the parachute riser line, a ±75g range accelerometer alined with the longitudinal axis of the vehicle, two ±5g range accelerometers mounted perpendicular to the longitudinal axis, an attitude reference system, and two cameras. The attitude reference system, commonly referred to as a gyro platform, was included to record payload motions in pitch, yaw, and roll during the test. One of the two cameras was mounted in a pod on the payload (fig. 2) and pointed aft to record parachute performance. The other camera was mounted in the nose of the payload and pointed forward such that it would provide data on payload motions relative to earth during the descent portion of the test. The tensiometer, accelerometer, and gyro platform measurements were telemetered to ground receiving stations where the data were recorded on magnetic tape. Camera film was obtained from the recovered payload. Correlation timing indications between telemetered data and camera film were obtained by means of coded time pulses.

In addition to the data-gathering instrumentation, the payload contained a C-band transponder to facilitate radar tracking and a beacon which could be located directionally by receiving equipment onboard an aircraft used in recovery operations. The payload

also contained two auxiliary parachutes which could be deployed by radio command at any time after payload separation if the performance of the test parachute (as observed on the real-time radar plotboard display) was such that the descent velocity was high and damage would most likely occur to the payload upon impact.

TEST PARACHUTE DESCRIPTION

The test parachute was a 30-foot (9.1-meter) nominal-diameter cross (or plus) design. As mentioned previously, results of an earlier test of a 25.2-foot (7.7-meter) nominal-diameter cross parachute are presented in appendix A, which also includes a detailed description of that parachute. The 30-foot (9.1-meter) cross parachute consisted of two rectangular panels crossed to form a "plus" shape, each panel having a width-length ratio of 0.264 as shown in figure 3. The center or crossover section was only a single thickness of cloth, although the load-carrying tapes from both panels were continuous across the center section. The test-parachute panel length was 39.3 feet (12.0 meters) and the width was 10.4 feet (3.2 meters); a total cloth area of 709 square feet (65.9 square meters) was thus provided. The cross parachute has no geometric open areas within the borders of the cloth material. (Note that this design has no vent at the center of the crown of the canopy.) The cloth area was taken as the reference area S_o and, therefore, the reference or nominal diameter D_o of the test parachute was 30 feet (9.1 meters). The general configuration of this parachute in flight is presented in figure 4.

The test parachute had nine suspension lines attached to each of the four panel ends for a total of 36 suspension lines. The lines were tubular braided dacron having a rated ultimate tensile strength of 550 pounds (2450 newtons) and a tested minimum ultimate tensile strength of 615 pounds (2740 newtons). The parachute canopy was fabricated of 2.60-ounce-per-square-yard (89-gram-per-square-meter) dacron cloth of dobby weave similar to parachute cloth per MIL-C-7350, type I. The canopy cloth had an ultimate tensile strength of 90 pounds per inch (160 newtons per centimeter) width. The canopy was reinforced with dacron load tapes which were extensions of the suspension lines and extended from end to end of the rectangular panels. There were a total of 18 load tapes, nine on each cross panel, each having a rated ultimate tensile strength of 750 pounds (3370 newtons). The warp threads in the canopy cloth were across the width of a panel. Therefore, the seams which joined the canopy cloth ran perpendicular to the load tapes. A dacron load tape of 1000-pound (4450-newton) rated tensile strength was sewn across the end of each panel in a manner similar to that of a skirt band.

The nine suspension lines extending from each panel end were grouped together at the lower end and sewn to a $1\frac{3}{4}$-inch (4.4-centimeter) wide dacron webbing of 7000-pound

(31 136 newtons) rated tensile strength. Each of the four suspension line webbings was then joined together at a point 22 inches (56 centimeters) below the attachment of the lines in order to form the upper riser.

The payload attachment system consisted of an upper riser, a swivel, and intermediate riser, a tensiometer, and a bridle. The total length of the attachment system was approximately $11\frac{1}{2}$ feet (3.5 meters). The parachute canopy, lines, and upper riser weighed 31.0 pounds (14.1 kilograms). The swivel, intermediate riser, tensiometer, and bridle weighed an additional 6.0 pounds (2.7 kilograms) for a total parachute system weight of 37.0 pounds (16.8 kilograms). Weight of the payload suspended from the parachute was 203 pounds (92.1 kilograms).

The parachute was pressure packed to a density of 40 pounds per cubic foot (640 kg/m^3) in a cylindrical bag of dacron canvas which was closed with a bag mouth tie. Prior to this flight test, the packed parachute was subjected to a heat cycle of 125° C for 120 hours (part of the proposed sterilization requirements for equipment to be used in interplanetary exploration) so that any effects of heat cycling would be present when the parachute was tested.

RESULTS AND DISCUSSION

A motion-picture film supplement L-994 has been prepared and is available on loan. A request card and a description of the film is included at the back of this document.

Test Data

The flight-test vehicle was launched at 9:45 a.m. m.d.t. on June 20, 1967, at White Sands Missile Range, New Mexico. Figure 5 presents a sketch of the flight sequence of events and the recorded times for significant events are listed on the right-hand side of the figure. Time histories of the altitude and relative velocity (total velocity with respect to the earth) for the first 360 seconds of the flight are shown in figure 6.

An Arcas meteorological sounding rocket was launched 25 hours prior to launch to measure upper-altitude winds (fig. 7) and also to measure the temperature for use in constructing the Mach number dynamic-pressure grids on the real-time radar display. Range scheduling limitations prevented launch of a sounding rocket shortly after the parachute test as was usually done for PEPP. Meteorological data from the rocket sounding were used for data-reduction purposes down to an altitude of 69 000 feet (21 kilometers). Below this altitude, data from a rawinsonde released 2 hours prior to launch were used when needed. Atmospheric density derived from the measured temperature profile is presented in figure 8.

The measured atmospheric data were used with radar track and telemetered acceleration and force data to determine the payload true airspeed, Mach number, and dynamic pressure which are presented in figures 9 and 10. The initiation of the deployment sequence or time of deployment was taken to be the time of mortar firing and is designated by $t' = 0$. The system altitude during the deployment time period, as determined by radar tracking, is presented in figure 11. Note that the payload was in the ascent portion of the flight trajectory during the sequence. As can be seen in figures 9, 10, and 11, parachute deployment was initiated at a true airspeed of 1670 fps (509 m/sec) ($M = 1.57$) and a dynamic pressure of 9.7 psf (460 N/m^2) and an altitude of 136 000 feet (41.5 kilometers) above mean sea level.

The true airspeed and Mach number at the time of mortar firing were determined from radar tracking data. Thereafter, the data presented in figure 9 were obtained from integrated tensiometer data. The slight increase in velocity at $t' = 0$ in figure 9 is a result of the reaction on the payload due to the firing of the mortar. Velocity decay evident at approximately 0.65 second resulted from the deceleration associated with the parachute inflation.

The time history of force measured by the tensiometer is presented in figure 12, beginning with the time of mortar firing. The first peak force of 725 pounds (3220 newtons) at 0.21 second is attributed to the full-length deployment of the bridle and the riser system. The second peak force of 1100 pounds (4900 newtons) at 0.44 second was the snatch force occurring at suspension-line stretch. The large sudden increase in force which begins at approximately 0.58 second is related to parachute inflation. The largest opening load occurred at 0.81 second and was 4255 pounds (18 930 newtons). Thereafter, the tensiometer force experienced a cyclic variation coinciding in time with panel "scissoring," that is, when the angle between any two adjacent panel arms oscillated between angles larger than and smaller than the design angle of 90°. It is known that the frequency of the force variation is approximately the same as the natural elastic frequency of the parachute suspension-line system. It is believed that the cyclic-force variation reflects an oscillation set up in the suspension-line system through a forcing function supplied by parachute drag. A detailed analysis of this elastic effect is outside the scope of the present report.

Time histories of acceleration obtained from the three orthogonally mounted accelerometers are presented in figure 13. The longitudinal accelerometer trace has a shape similar to that obtained from the tensiometer force time history, as would be expected. The largest deceleration recorded was 22.3g and occurred at 0.81 second; this time corresponded with the time of occurrence of the largest tensiometer force recorded. Acceleration time histories for the transverse and normal accelerometers, both of

which were located on the payload spin axis, indicate that the payload did not remain alined with the flight path.

As mentioned previously, onboard instrumentation included an aft-looking camera, a forward-looking camera, and an attitude reference system (gyro platform). The aft camera film data were used in conjunction with the gyro platform data to determine the pitch, yaw, and roll stability of the parachute during the deceleration period and during terminal descent. The aft camera had a frame rate of 32.2 frames per second and provided 112 seconds of film data beginning 1 second prior to mortar fire. The gyro platform provided payload pitch, yaw, and roll attitude data for 360 seconds. Gyro data are measured relative to the uncaged position of the platform on the launcher, which is normally the vehicle position at lift-off. However, to counter the effects of high-altitude winds which can cause the platform to exceed its yaw operating limits and tumble (for example, ref. 3), an operational procedure of temporarily offsetting the launcher from the lift-off position and uncaging the gyro platform at this position was formulated and used for this flight. The results of this procedure were successful, and continuous data were obtained for the entire test period. A brief discussion of this operational method and transformation equations relating the raw gyro data to displacements from the local vertical during descent are set forth in appendix B.

Parachute Performance

Inflation characteristics.- The time from deployment mortar ignition to suspension-line stretch was 0.44 second; thus, an average mortar ejection velocity of 115 ft/sec (35 m/sec) was achieved (based on the total suspension system length of 50.8 feet (15.5 meters)).

The increase in parachute projected area associated with canopy inflation could not be plotted because of the fact that a filmy coating was deposited on the camera lens sometime during the flight; thus detailed measurement of canopy projected area was impossible. However, the total time increment over which inflation occurred could be obtained from the film data. Figure 14(a) presents several frames of onboard camera photographs. Canopy projected area increase began at approximately 0.58 second and a first full inflation appears to have occurred at 0.77 second. Immediately thereafter, panel arm scissoring set in, as can be seen in figure 14(b). This motion persisted throughout the test period; the amplitude was greatest during the 7-second high-deceleration period and decreased to small values during descent, as shown in figure 14(c). From analyzing the film data, it was determined that during the time interval from $t' = 1.00$ to $t' \approx 2.00$ seconds, the symmetrical cross shape was momentarily attained nine times. This frequency coincides with the frequency of force variation on the tensiometer record. It is believed that the erratic oscillations of individual panel

arms resulted from the failure of this particular cross design, in conjunction with its suspension-line system, to maintain a steady flow field around the canopy.

In addition to the scissoring, it was noted that the panel ends intermittently folded in toward the center of the canopy. In the region near apogee, one panel folded inward almost completely.

Drag efficiency.- The axial-force coefficient $C_{A,o}$ based on the area of the canopy cloth S_o is presented in figure 15 for the deceleration period. In addition to the time scale, a Mach number scale is also shown. In previous PEPP reports (refs. 2 to 5) the calculated force cofficient was referred to as a drag coefficient $C_{D,o}$. This designation was based on the assumption that the payload-parachute system acted as a quasi-rigid body so that the drag force acting on the parachute was transmitted through the suspension lines, riser system, and tensiometer to the payload essentially unaltered. However, for the presently reported test, canopy shape changes excited the natural elastic frequency of the suspension lines; as a result, the tensiometer recording included the effects of elastic oscillations in addition to the drag force provided by the canopy. The axial-force coefficient was calculated by using the density data from figure 8, the true airspeed data from figure 9, and the tensiometer force data from figure 12. The equation used to determine this coefficient is as follows:

$$C_{A,o} = \frac{m_{total}}{m_{payload}} \frac{T}{q_\infty S_o}$$

Although the variations found in figure 15 are large, an average value of 0.69 is exhibited and thus indicates that this decelerator was an effective drag-producing device. The average uncertainty in $C_{A,o}$ based on a first-order error analysis using 3-percent velocity error, 3-percent density error, and 100-pound (444.8-newton) tensiometer error, was estimated to be ±0.04.

Values of the "effective" drag coefficient based on the vertical components of velocity and acceleration during the descent portion of the flight were computed by using the following equation:

$$(C_{D,o})_{eff} = \frac{2m_{total}}{\rho_\infty \dot{Z}_E^2 S_o}\left(g - \ddot{Z}_E\right)$$

(In refs. 3 and 5, the acceleration term was not included because its contribution to $(C_{D,o})_{eff}$ was negligible.) The effective drag coefficient and vertical descent velocity are presented in figure 16 as a function of altitude. An average value of 0.78 was attained over the altitude range from 18 000 to 120 000 feet (5.5 to 36.6 kilometers). The estimated uncertainty in this average drag coefficient is ±0.04 using 3-percent velocity error, 3-percent density error, and 10-percent acceleration error.

Stability.- At time of mortar firing, the payload roll rate was 5.0 revolutions per second. Analysis of the aft camera film revealed that the parachute canopy retained very little of this rolling motion once the canopy had inflated. This effect is shown by figure 17 which presents a comparison between the payload roll rate (gyro data) and the relative roll rate between the payload and the parachute (camera data) during the initial high-deceleration portion of the test. Over the data period shown, the net canopy roll was 0.5 revolution and was in the same direction as that of the payload roll. It should be noted that this was the first test in the series where a swivel was inserted in the parachute riser line. The swivel was included to restrict the rolling motion to the payload, bridle, and intermediate riser, and to prevent the possibility of the suspension lines twisting together, as had occurred during the flight test reported in reference 4. The swivel, of course, reduced payload roll damping from that experienced during the earlier rocket-launched PEPP tests. (See refs. 3 to 5.) As a result, payload precession produced large pitch and yaw displacements about the flight path which became as high as 62° near apogee. Figure 18 presents a comparison of the payload pitch and yaw time histories with the relative angular displacement between the payload and the parachute as determined from aft camera film during that portion of the test immediately following deployment. Note that the values of θ_g and ψ_g at $t' = 0$ are measurements of the net pitch and yaw which the payload underwent from the time of gyro uncaging to the time of mortar firing. The dashed lines, $\overline{\theta}_g$ and $\overline{\psi}_g$, give an indication of the pitch and yaw motion of the payload-parachute system; the oscillatory portion of θ_g and ψ_g indicates payload precession about the parachute center line. The high-frequency content of the camera data shows that, in addition to the relatively smooth payload precession motion present, canopy pitch-yaw oscillations were present and were most likely a result of the previously mentioned canopy-shape variations.

During descent, canopy-shape oscillations had reduced to small amplitudes and the stability of the system greatly improved. Payload motions during a descent portion of the flight were obtained by transforming the gyro platform data to an axis system containing the local vertical. (See appendix B.) The body-axis and Euler angle system used are also shown in appendix B. The angles ψ_E and θ_E are measures of the pitching and yawing angular displacements of the payload and the resultant angle δ_E is the total pitch-yaw displacement of the longitudinal axis from the local vertical. Time histories of ψ_E and θ_E and $|\delta_E|$ are shown in figure 19 for a time period from $t' = 50$ to $t' = 112$ seconds which corresponds to an altitude range from 134 000 to 116 000 feet (40.8 to 35.4 kilometers). It can be seen from this figure that both ψ_E and θ_E contain two rather distinct frequencies, approximately 1.2 cps and 0.2 cps. The high-frequency content of these parameters is generally 90° out of phase, and it was determined by analyzing the aft-camera film data that this motion was payload coning about the parachute center line. Long-period oscillations result from the combined

payload-parachute system acting in a manner similar to a pendulum. As can be seen from figure 19, the total angular displacement $|\delta_E|$ was never greater than 21^o and exhibited an average value of less than 10^o during the time interval shown. A large portion of $|\delta_E|$ results from the payload coning about the parachute center line. This latter motion would be induced by the payload rolling motion (which was approximately 1.2 cps during this time interval) if there existed an asymmetry among the three legs of the bridle system. It appears from this result that for specific applications where it is desirous to minimize δ_E, consideration should be given to reduce payload roll and to the design of a payload attachment system to minimize oscillations.

Parachute damage analysis.- A postflight inspection of the recovered parachute revealed that no apparent damage was incurred by the test parachute during the flight test. A photograph of the payload and parachute system taken at the recovery site is presented in figure 20.

CONCLUSIONS

The 30-foot (9.1-meter) nominal-diameter cross-type parachute with a cloth area (reference area) of 709 square feet (65.9 square meters) and a width-to-length ratio of 0.264 was flight tested with a 203-pound (92.1-kilogram) instrumented payload. Mortar deployment occurred at an altitude of 136 000 feet (41.5 kilometers) at a Mach number of 1.57 and a dynamic pressure of 9.7 pounds per square foot (460 newtons per square meter). Based on the performance of the test parachute, the following conclusions are drawn:

1. The mortar deployment system operated correctly and the time to suspension-line stretch was 0.44 second with a resulting snatch force of 1100 pounds (4900 newtons).

2. Canopy inflation began at 0.58 second and a first full inflation was achieved at approximately 0.77 second.

3. The maximum opening load recorded occurred at 0.81 second and was 4255 pounds (18 930 newtons).

4. The canopy did not maintain the proper cross or plus shape at any time during the test period; violent "scissoring" occurred during the high-deceleration period, but reduced to smaller amplitudes during descent.

5. The parachute exhibited an average axial-force coefficient of 0.69 during the high-deceleration period and an effective drag coefficient of 0.78 during descent.

6. During the system descent from 134 000 to 116 000 feet (40.8 to 35.4 kilometers), payload resultant pitch-yaw motions varied between 0^{o} and 21^{o} but averaged less than 10^{o}.

Langley Research Center,
National Aeronautics and Space Administration,
Langley Station, Hampton, Va., February 15, 1968,
709-08-00-01-23.

APPENDIX A

EARLIER FLIGHT TEST OF A CROSS PARACHUTE

A 25.2-foot (7.7-meter) nominal-diameter cross parachute was flight tested on February 28, 1967, at White Sands Missile Range as part of the PEPP test series. The test parachute deployed properly from the payload, but structural failure of the suspension-line risers during the canopy opening process resulted in loss of the parachute and all performance data for the remainder of the flight. Although limited parachute performance data were obtained from this flight test, information concerning inflation time and opening loads was obtained. This appendix is included in this report in order to present the data which are available. A detailed description of the test parachute is presented along with an analysis of the flight data obtained.

Test Parachute Description

The parachute tested in February 1967 was a cross (or plus) design having a panel width-length ratio of 0.333 as shown in figure 21. The length of each panel was 30 feet (9.1 meters) and the width 10 feet (3.0 meters), with a resultant total cloth area of 500 square feet (46 square meter). Based on cloth area alone, the parachute had a nominal diameter D_o of 25.2 feet (7.7 meters).

The parachute canopy was fabricated of 1.3-ounce-per-square-yard (44-gram-per-square-meter) dacron cloth of rip-stop pattern. The canopy cloth was reinforced with dacron load tapes which traversed the cross panels from end to end. These load tapes were equally spaced, seven being on each cross panel. In the center section of the canopy, the load tapes crossed in a grid pattern; however, there was not a double thickness of cloth in this area. As was the case for the other cross parachute presented in this report, the canopy cloth was positioned such that the direction of the warp threads was across the width of a panel. Therefore, the seams which joined the canopy cloth ran perpendicular to the load tapes. A dacron load tape was also located across the ends of each of the panels, similar to a skirt band. The dacron load tapes used for canopy reinforcement were 9/16 inch (1.4 centimeter) wide and had a nominal tensile strength of 450 pounds (2000 newtons).

The 25.2-foot (7.7-meter) D_o parachute had seven 550-pound (2450-newton) tensile strength dacron suspension lines attached to each end of the four panel ends for a total of 28 suspension lines. The seven suspension lines from an end of a canopy cross panel were grouped together at the lower end and sewn to a $1\frac{1}{2}$-inch (3.8-centimeter) wide dacron webbing having a nominal tensile strength of 1500 pounds (6700 newtons).

The four webbings were joined together at a point $17\frac{1}{2}$ inches (44.5 centimeters) below the attachment of the suspension lines. At the point where the four webbings joined, an additional piece of webbing (generally referred to as a "keeper") was wrapped around them and sewn in place to form a confluence point. The distance from the canopy skirt to this confluence point was 30 feet (9.1 meters), a distance equal to the length of a canopy cross panel. The suspension-line attachment webbings extended about $3\frac{1}{2}$ inches (8.9 centimeters) below the confluence point to form an attachment point for the riser system.

The payload attachment system consisted of an upper riser, a disconnect link, an intermediate riser, a tensiometer, and a bridle. The total length of the attachment system was approximately 13 feet (4.0 meters). The total weight of the parachute system attached to the payload was 18.42 pounds (8.34 kilograms), 11.25 pounds (5.10 kilograms) of which were provided by the canopy, suspension lines, and line attachment webbings. The weight of the suspended payload was approximately 200 pounds (91 kilograms).

Performance Analysis

Mortar firing to initiate deployment of the test parachute for the February flight test occurred when the payload was at a Mach number of 1.57 and an altitude of 132 500 feet (40.4 kilometers); the dynamic pressure experienced at this time was 9.9 pounds per square foot (470 newtons per square meter). The longitudinal accelerometer time history is presented in figure 22 for a time period subsequent to mortar firing. The first peak of 4.7g which occurred at $t' = 0.24$ second corresponded to full-length deployment of the bridle and risers. The 4.8g acceleration shown at 0.33 second in figure 22 is the snatch force loading associated with suspension-line stretch. It is to be noted that these peaks are to be expected for the mortar deployment method used. The deceleration loading associated with parachute inflation began at $t' = 0.45$ second and reached a maximum of 16.35g at $t' = 0.52$ second, after which the deceleration dropped to zero because of separation of the test parachute from the payload.

Figure 23 presents the parachute projected-area increase with time as determined from onboard camera film. Selected frames from this film are presented in figure 24. Parachute deployment and inflation are shown in figure 24(a), whereas figure 24(b) shows the parachute after it has separated from the payload. Note that there is no tension in the three attachment webbings (payload bridle) in figure 24(b).

The primary structural failure in the parachute system occurred at the lower end or confluence point of the $1\frac{1}{2}$-inch (3.8-centimeter) wide dacron webbings which had the suspension lines sewn to them. (See fig. 25.) As mentioned previously, these four webbings had a rated tensile strength of 1500 pounds (6700 newtons) each for a total

rated strength of 6000 pounds (27 000 newtons); however, the total allowable load would be somewhat less, primarily because of the reduced joint efficiency at the confluence point caused by the sewing of the webbings. At the time of failure, the tension in the suspension system was approximately 3300 pounds (15 000 newtons) based on the maximum accelerometer recording.

Although the parachute opening load as recorded for the test parachute was of the same magnitude as those of two parachute designs of about 30-foot (9.1-meter) D_o tested previously (refs. 2 and 4), the canopy inflation rate and the rate of load buildup was much more rapid. It is concluded that the tensile strength of the suspension-line webbings was insufficient to cope with the rapid load buildup, and structural failure resulted.

APPENDIX B

NOTES ON GYRO PLATFORM OPERATIONAL OFFSET PROCEDURE AND DATA REDUCTION

It is known that a payload-parachute system in free flight will respond to the wind by pitching or yawing in the direction from which the wind is blowing. The wind effects on the parachute systems tested in the PEPP series appear to be greatest near the apogee region of the flight profile since the parachute velocity is rapidly approaching a minimum value on the order of 150 ft/sec (46 m/sec) and wind velocity can be of a comparable order of magnitude.

For the PEPP test reported in the main body of this report, a meteorological sounding rocket launched 25 hours prior to the parachute flight test measured wind in the expected apogee region to be generally out of the northeast. (See fig. 7.) Since the required launch azimuth for the two-stage launch vehicle was 340° from the north, it was anticipated prior to launch that some yawing motion toward the northeast would result when the parachute system approached apogee. It was also known from a previous PEPP test (ref. 4) that upon parachute deployment, the spinning payload would precess at large angles about its trim attitude. The combination of wind-induced yaw and payload precession produced a yaw angle greater than 85° at one time during the test of reference 4, and caused the gyro platform (which has mechanical stops at that position) to tumble. As a result, no gyro data were available beyond apogee for that flight test and no stability characteristics were ascertained for the steady-state descent portion of that flight. It was anticipated prior to this test that a similar loss of gyro data would result if the standard procedure of uncaging the gyro at the vehicle lift-off position was used. It was therefore decided to perform the uncaging function while the vehicle was at a preliminary azimuth setting of 20° and its final elevation of 85.4°, and rotate the launcher about the local vertical to the launch azimuth of 340°. In this manner, a 40° bias would be present in the yaw plane when the payload-parachute system was in a horizontal position at apogee. The effect of yawing into the wind would then be to return the gyro yaw position toward its zero reference. It was believed that as a result of this procedure, precession angles approaching the $\pm 85^{\circ}$ limit could be tolerated. The results of this procedure were successful, and gyro data were available for the entire test period.

To obtain information on the payload-parachute system pitch-yaw motions during descent, it is necessary to transform the raw gyro data to an earth-fixed coordinate

system containing the local vertical. This transformation can be accomplished through the following considerations:

(1) The transformation equations relating the position of the launch vehicle (and gyro platform) at lift-off to the earth-fixed axis system shown in sketch (a) are:

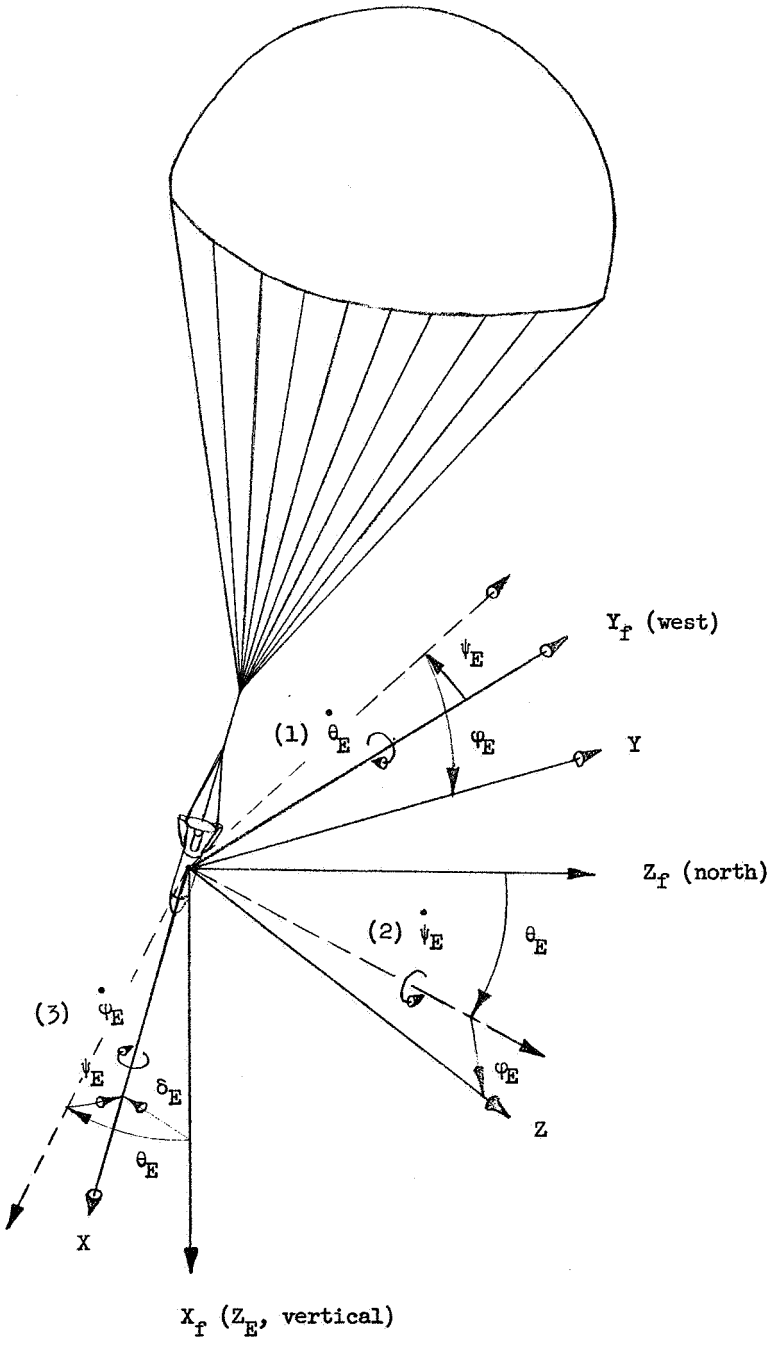

APPENDIX B

$$\begin{pmatrix} X_l \\ Y_l \\ Z_l \end{pmatrix} = H \begin{pmatrix} X_f \\ Y_f \\ Z_f \end{pmatrix} \tag{B1}$$

where

$$H = \begin{bmatrix} \cos \Gamma & \sin \Gamma \sin \Lambda & -\sin \Gamma \cos \Lambda \\ 0 & \cos \Lambda & \sin \Lambda \\ \sin \Gamma & -\cos \Gamma \sin \Lambda & \cos \Gamma \cos \Lambda \end{bmatrix}$$

and

Λ launch azimuth

Γ -(launch elevation + 90^{o})

(Note that all coordinate systems used in this appendix are right-handed systems and the positive sense of angles are such that rotations about any axis are clockwise when viewed along a positive axis. Note that the symbol Z_E is introduced on the sketch to be consistent with definition of $(C_{D,o})_{eff}$ used herein and in refs. 2 to 5.)

(2) The lift-off attitude is related to the zero positions of the gyro through the initial pitch, yaw, and roll readings at lift-off. This initial reading results from the offset procedure of rotating the launcher and from drift caused by the earth's rotation and random sources during the final phases of the countdown. Since platform construction dictates an Euler angle sequence of pitch, yaw, and roll, in that order, the transformation relating the two axis systems will have the same form as that derived in reference 3 for any gyro motion relative to the uncaged or zero readings. These transformation equations can be written as follows:

$$\begin{pmatrix} X_l \\ Y_l \\ Z_l \end{pmatrix} = J \begin{pmatrix} X_o \\ Y_o \\ Z_o \end{pmatrix} \tag{B2}$$

where

$$J = \begin{bmatrix} \cos\psi_o \cos\theta_o & \sin\psi_o & -\cos\psi_o \sin\theta_o \\ -\cos\varphi_o \sin\psi_o \cos\theta_o + \sin\varphi_o \sin\theta_o & \cos\psi_o \cos\varphi_o & \cos\varphi_o \sin\psi_o \sin\theta_o + \sin\varphi_o \cos\theta_o \\ \sin\varphi_o \sin\psi_o \cos\theta_o + \cos\varphi_o \sin\theta_o & -\sin\varphi_o \cos\psi_o & -\sin\varphi_o \sin\theta_o \sin\psi_o + \cos\varphi_o \cos\theta_o \end{bmatrix}$$

and θ_o, ψ_o, and φ_o are the initial platform readings at lift-off.

(3) The payload body-axis system at any time during the flight is related to the gyro zero or inertial reference through the general platform transformation

$$\begin{pmatrix} X \\ Y \\ Z \end{pmatrix} = K \begin{pmatrix} X_o \\ Y_o \\ Z_o \end{pmatrix} \tag{B3}$$

where

$$K = \begin{bmatrix} \cos\psi_g \cos\theta_g & \sin\psi_g & -\cos\psi_g \sin\theta_g \\ -\cos\varphi_g \sin\psi_g \cos\theta_g + \sin\varphi_g \sin\theta_g & \cos\psi_g \cos\varphi_g & \cos\varphi_g \sin\psi_g \sin\theta_g + \sin\varphi_g \cos\theta_g \\ \sin\varphi_g \sin\psi_g \cos\theta_g + \cos\varphi_g \sin\theta_g & -\sin\varphi_g \cos\psi_g & -\sin\varphi_g \sin\theta_g \sin\psi_g + \cos\varphi_g \cos\theta_g \end{bmatrix}$$

and θ_g, ψ_g, and φ_g are the raw data or those values recorded during the flight test.

(4) The payload body-axis system can also be related to the earth-fixed axis system through any Euler angle system. If the pitch, yaw, and roll sequence is chosen for convenience, the transformation equations can then be written as

APPENDIX B

$$\begin{pmatrix} X \\ Y \\ Z \end{pmatrix} = L \begin{pmatrix} X_f \\ Y_f \\ Z_f \end{pmatrix} \tag{B4}$$

where

$$L = \begin{bmatrix} \cos\psi_E \cos\theta_E & \sin\psi_E & -\cos\psi_E \sin\theta_E \\ -\cos\varphi_E \sin\psi_E \cos\theta_E + \sin\varphi_E \sin\theta_E & \cos\psi_E \cos\varphi_E & \cos\varphi_E \sin\psi_E \sin\theta_E + \sin\varphi_E \cos\theta_E \\ \sin\varphi_E \sin\psi_E \cos\theta_E + \cos\varphi_E \sin\theta_E & -\sin\varphi_E \cos\psi_E & -\sin\varphi_E \sin\theta_E \sin\psi_E + \cos\varphi_E \cos\theta_E \end{bmatrix}$$

and θ_E, ψ_E, and φ_E are shown in the sketch.

Through mathematical substitution, the four matrices can be related in the following form:

$$L = KJ^{-1}H \tag{B5}$$

where J^{-1} is the inverse to J which is identical to the transposed matrix in this case and can be obtained by interchanging the rows of the matrix array with the columns.

If the matrix multiplication indicated by equation (B5) is performed and the corresponding matrix elements are equated, it is found that

$$\psi_E = \sin^{-1}\left(l_{12}\right) \tag{B6a}$$

$$\psi_E = \sin^{-1}\left[\left(j_{11}h_{12} + j_{21}h_{22} + j_{31}h_{32}\right)k_{11} + \left(j_{12}h_{12} + j_{22}h_{22} + j_{32}h_{32}\right)k_{12} + \left(j_{13}h_{12} + j_{23}h_{22} + j_{33}h_{32}\right)k_{13}\right] \tag{B6b}$$

and

$$\theta_E = -\tan^{-1}\frac{l_{13}}{l_{11}} \tag{B7a}$$

$$\theta_E = -\tan^{-1} \frac{(j_{11}h_{13} + j_{21}h_{23} + j_{31}h_{33})k_{11} + (j_{12}h_{13} + j_{22}h_{23} + j_{32}h_{33})k_{12} + (j_{13}h_{13} + j_{23}h_{23} + j_{33}h_{33})k_{13}}{(j_{11}h_{11} + j_{21}h_{21} + j_{31}h_{31})k_{11} + (j_{12}h_{11} + j_{22}h_{21} + j_{32}h_{31})k_{12} + (j_{13}h_{11} + j_{23}h_{21} + j_{33}h_{31})k_{13}} \quad \text{(B7b)}$$

and

$$\varphi_E = -\tan^{-1} \frac{l_{32}}{l_{22}} \quad \text{(B8a)}$$

$$\varphi_E = -\tan^{-1} \frac{(j_{11}h_{12} + j_{21}h_{22} + j_{31}h_{32})k_{31} + (j_{12}h_{12} + j_{22}h_{22} + j_{32}h_{32})k_{32} + (j_{13}h_{12} + j_{23}h_{22} + j_{33}h_{32})k_{33}}{(j_{11}h_{12} + j_{21}h_{22} + j_{31}h_{32})k_{21} + (j_{12}h_{12} + j_{22}h_{22} + j_{32}h_{32})k_{22} + (j_{13}h_{12} + j_{23}h_{22} + j_{33}h_{32})k_{23}} \quad \text{(B8b)}$$

Equations (B6), (B7), and (B8) relate the gyro flight data and initial known conditions to a set of angles which are more meaningful in determining the pitch-yaw stability of a descending parachute system.

REFERENCES

1. McFall, John C., Jr.; and Murrow, Harold N.: Parachute Testing at Altitudes Between 30 and 90 Kilometers. AIAA Aerodynamic Deceleration Systems Conference, Sept. 1966, pp. 116-121.

2. Whitlock, Charles H.; Bendura, Richard J.; and Coltrane, Lucille C.: Performance of a 26-Meter-Diameter Ringsail Parachute in a Simulated Martian Environment. NASA TM X-1356, 1967.

3. Preisser, John S.; Eckstrom, Clinton V.; and Murrow, Harold N.: Flight Test of a 31.2-Foot-Diameter Modified Ringsail Parachute Deployed at a Mach Number of 1.39 and a Dynamic Pressure of 11 Pounds Per Square Foot. NASA TM X-1414, 1967.

4. Eckstrom, Clinton V.; Murrow, Harold N.; and Preisser, John S.: Flight Test of a 40-Foot-Nominal-Diameter Modified Ringsail Parachute Deployed at a Mach Number of 1.64 and a Dynamic Pressure of 9.1 Pounds Per Square Foot. NASA TM X-1484, 1967.

5. Eckstrom, Clinton V.; and Preisser, John S.: Flight Test of a 30-Foot-Nominal-Diameter Disk-Gap-Band Parachute Deployed at a Mach Number of 1.56 and a Dynamic Pressure of 11.4 Pounds Per Square Foot. NASA TM X-1451, 1967.

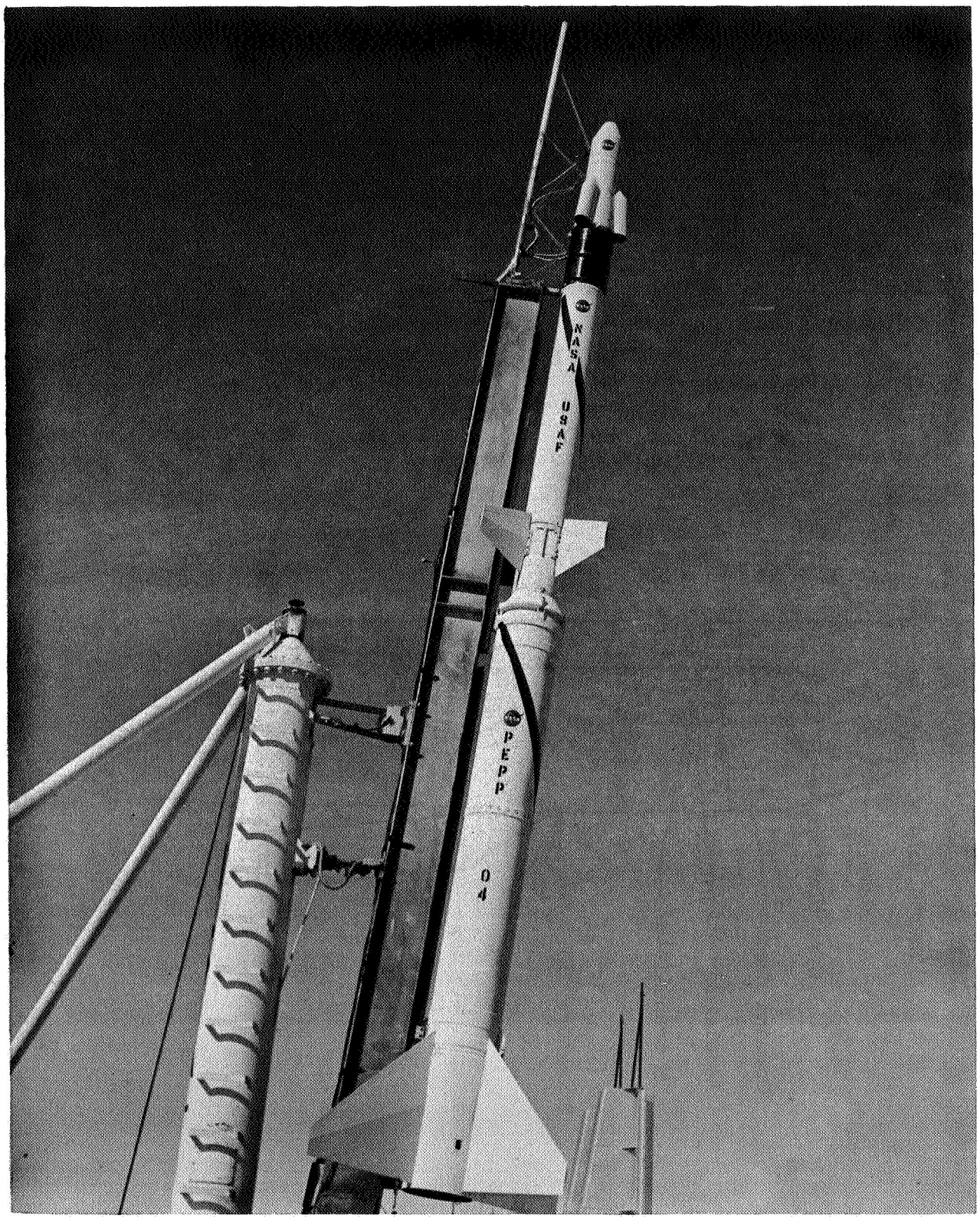

Figure 1.- Vehicle configuration. L-68-831

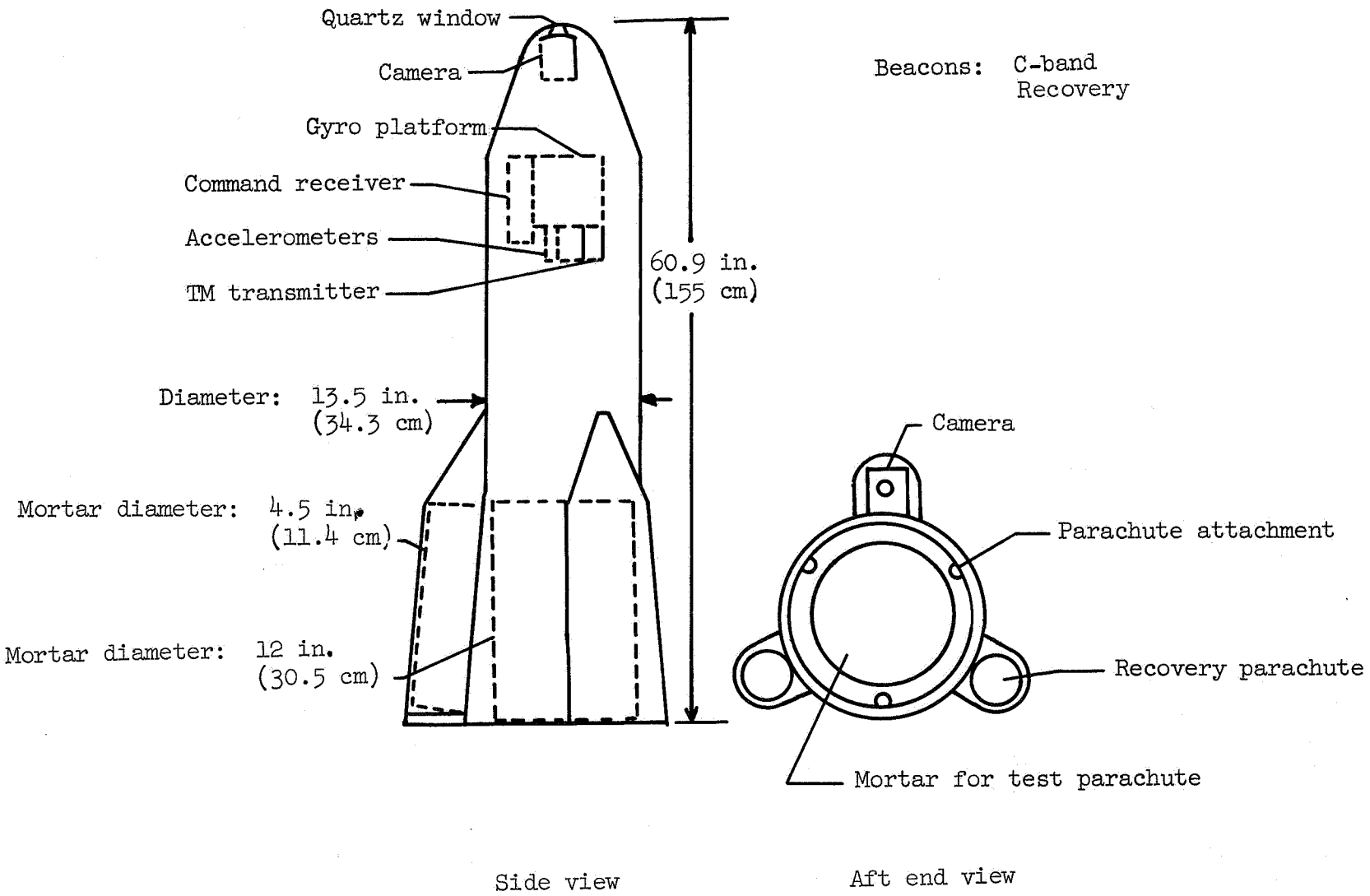

Figure 2.- Test payload.

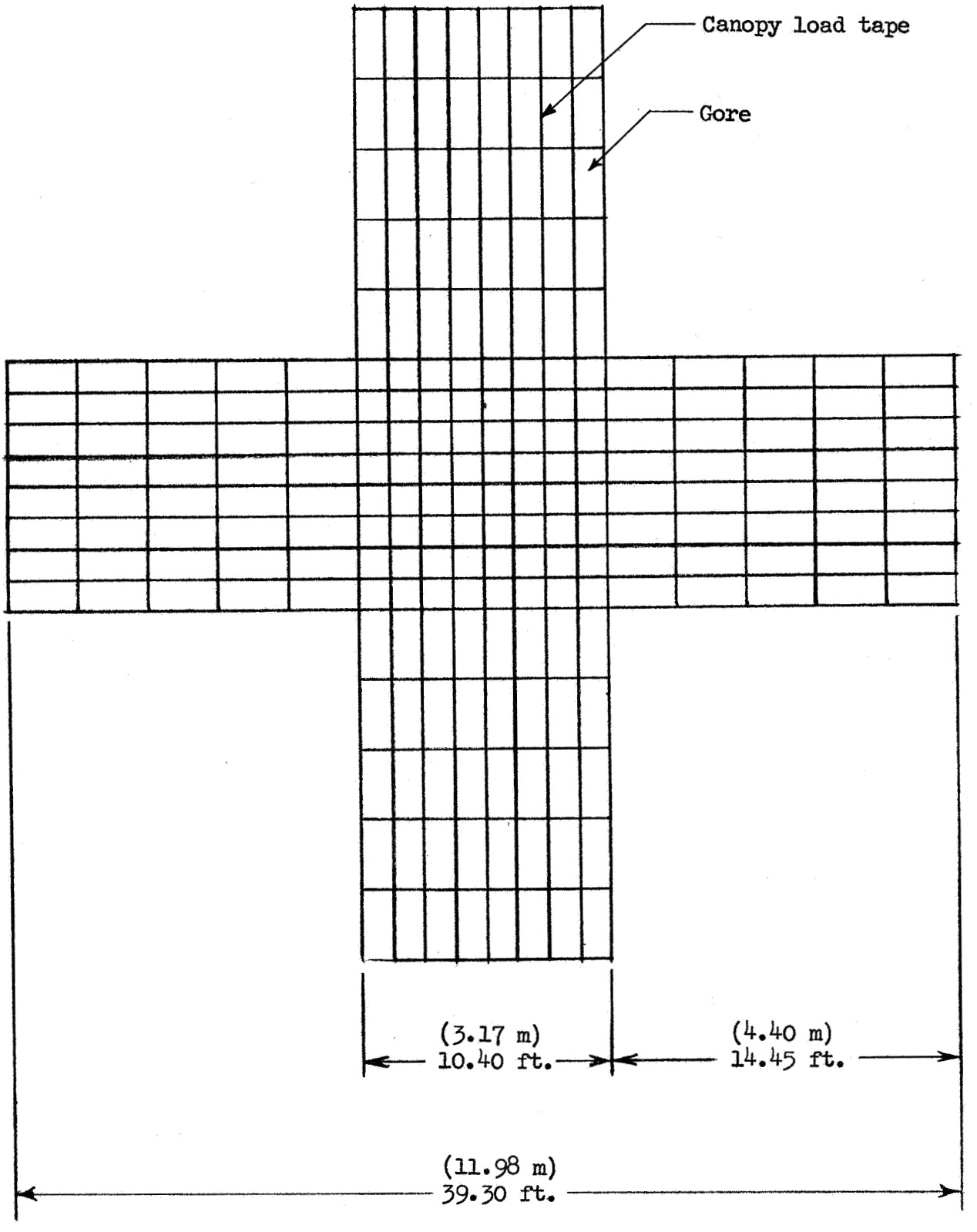

Figure 3.- Canopy layout of 0.264 width-length ratio cross parachute.

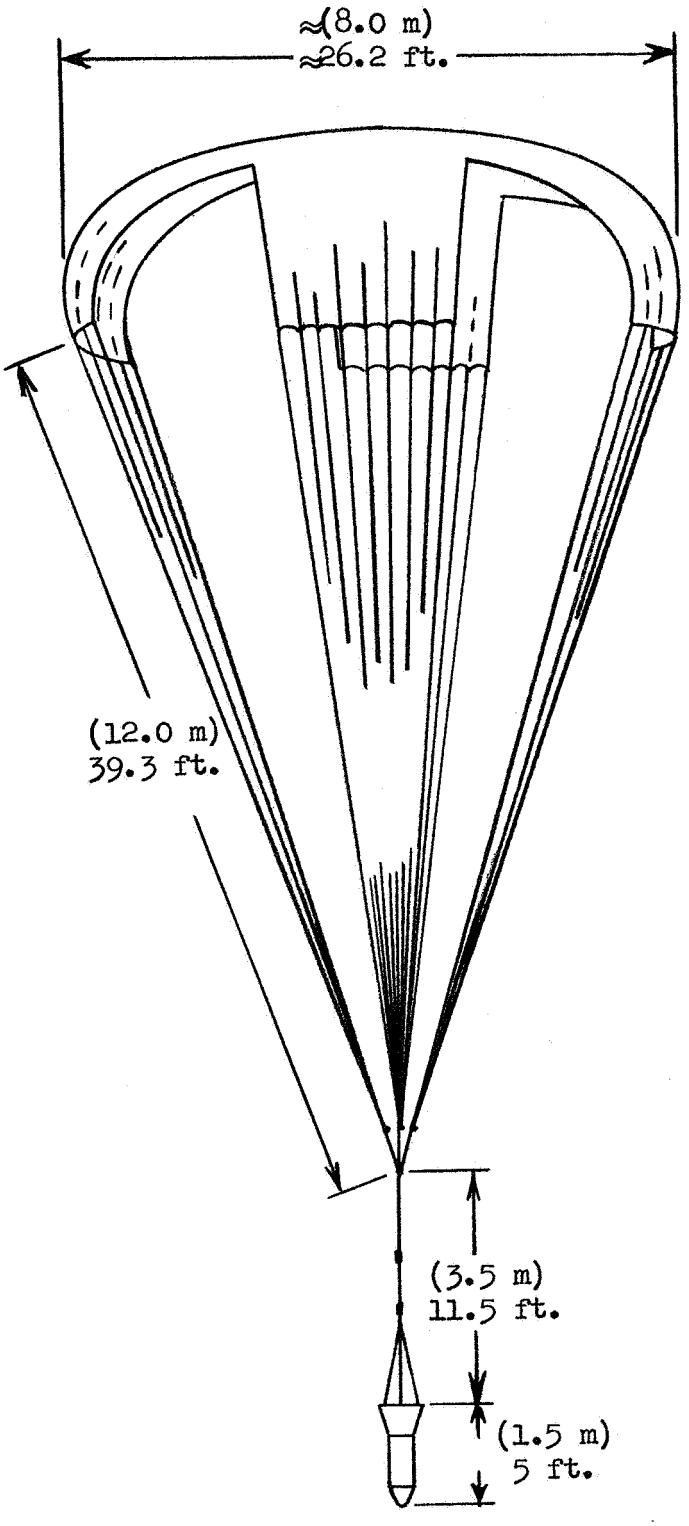

Figure 4.- General flight configuration.

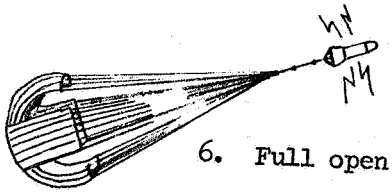

6. Full open

5. Mortar ejection of parachute

4. Radio command to start cameras and programer

3. Payload separation

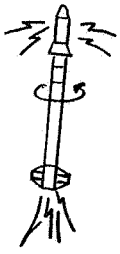

2. Second-stage ignition and vehicle spin-up

Event	Time, t, sec
1	0
2	15.30
3	54.39
4	59.88
5	60.56
6	61.33
7	2412

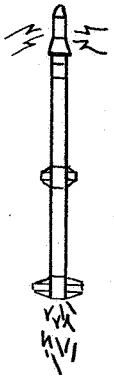

1. Vehicle lift off

7. Impact

Figure 5.- Flight sequence of events.

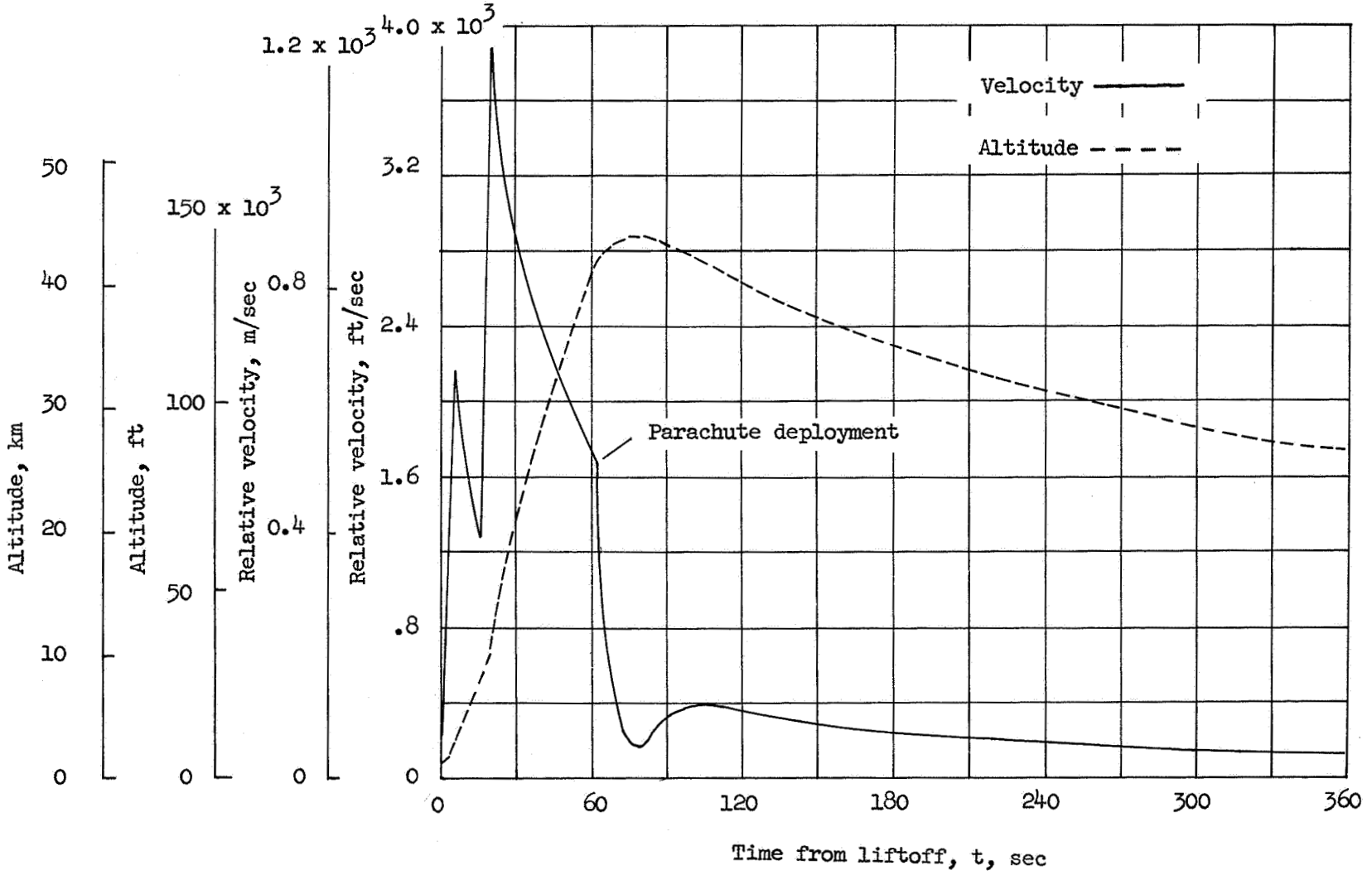

Figure 6.- Altitude and relative velocity time histories.

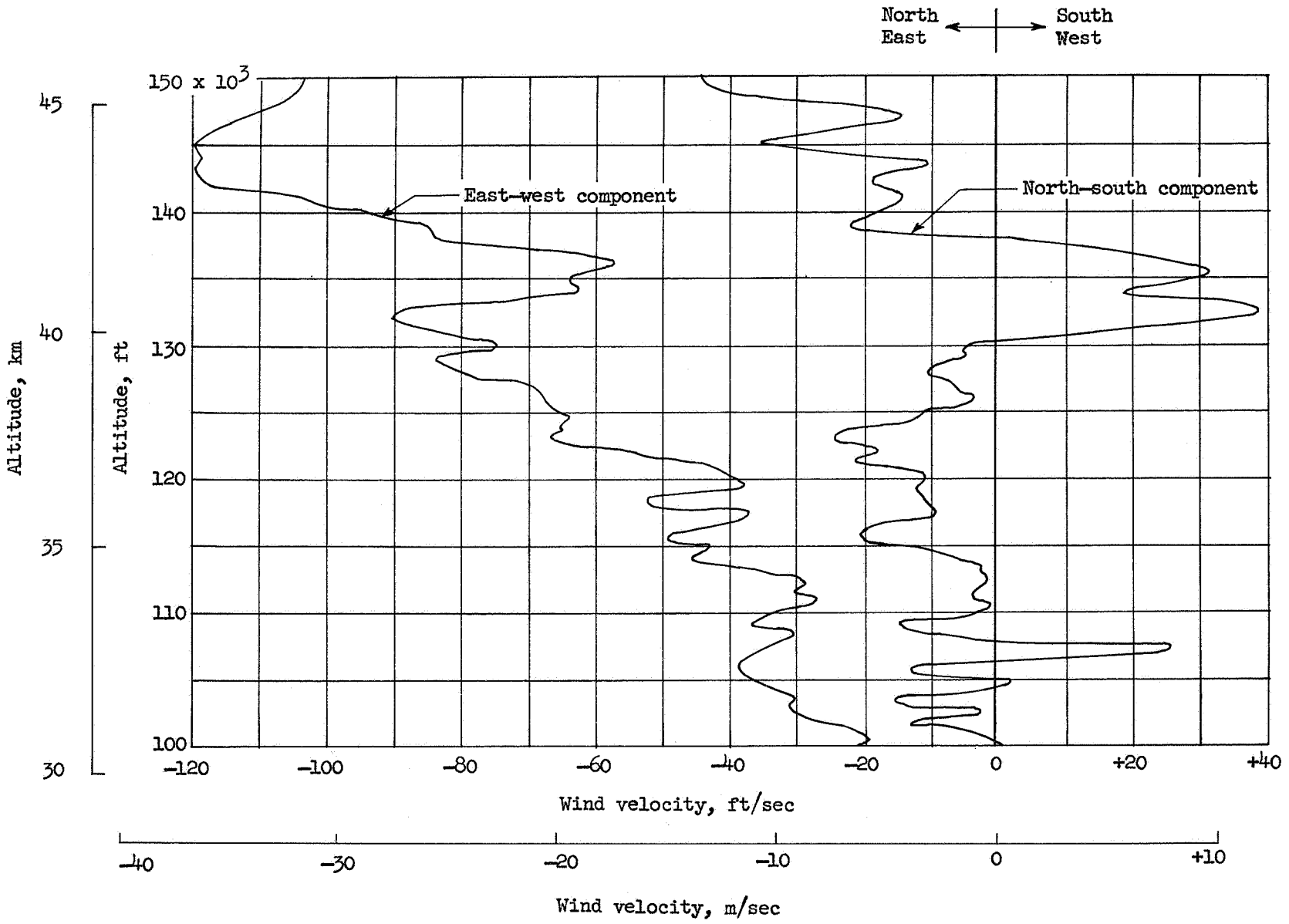

Figure 7.- Wind-velocity profile in north-south and east-west components.

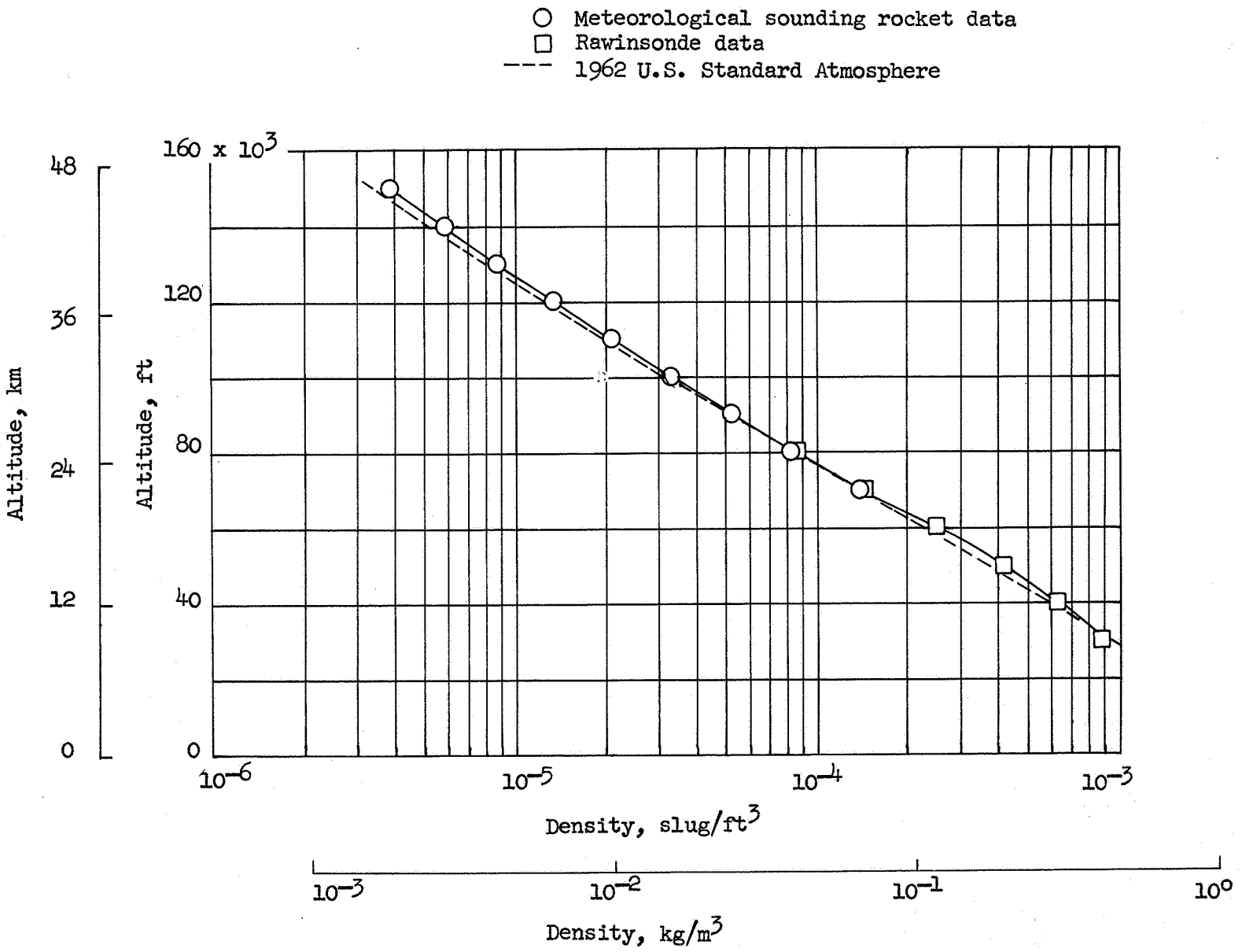

Figure 8.- Atmospheric density profile.

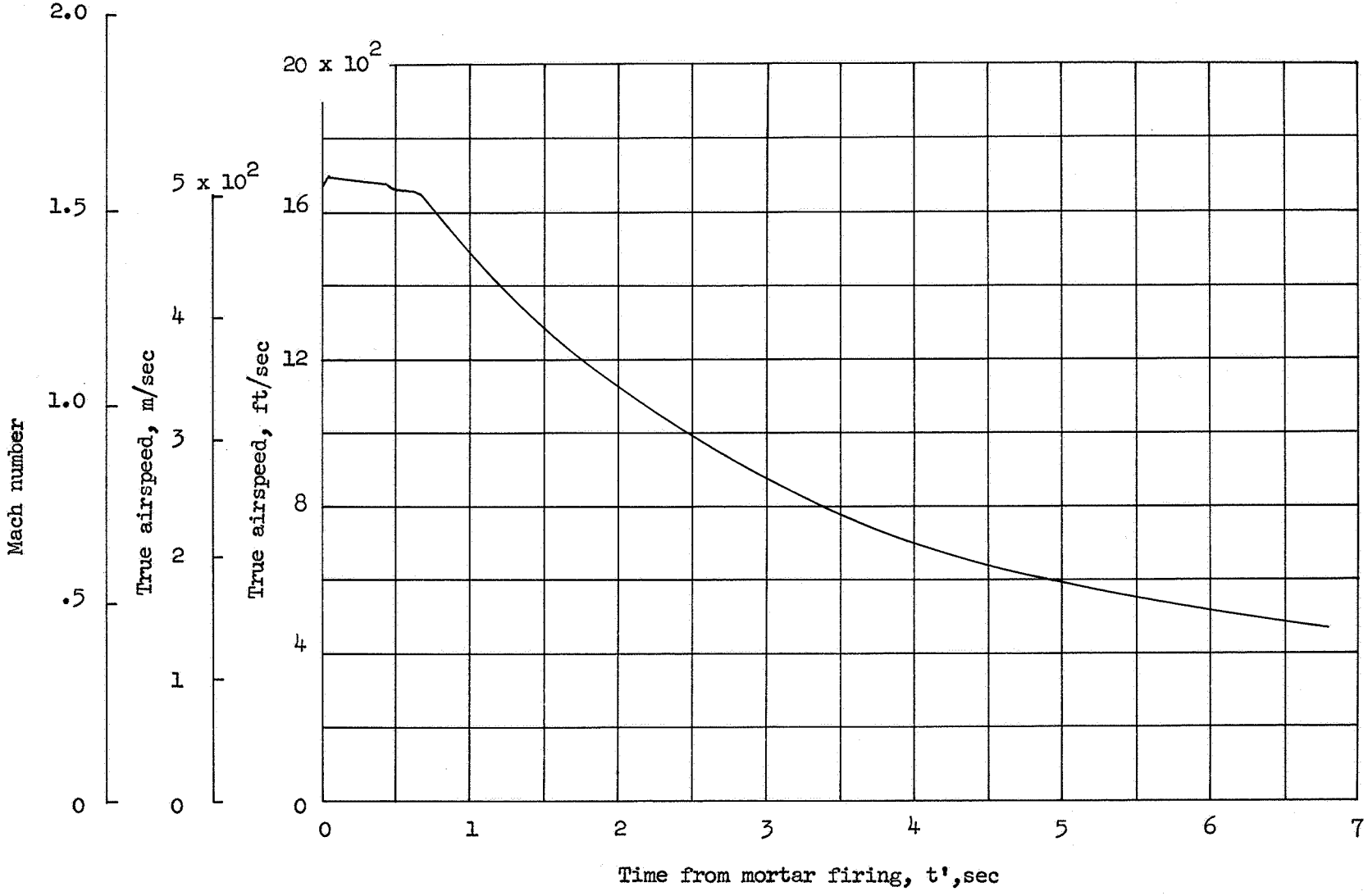

Figure 9.- True airspeed and Mach number decay with time.

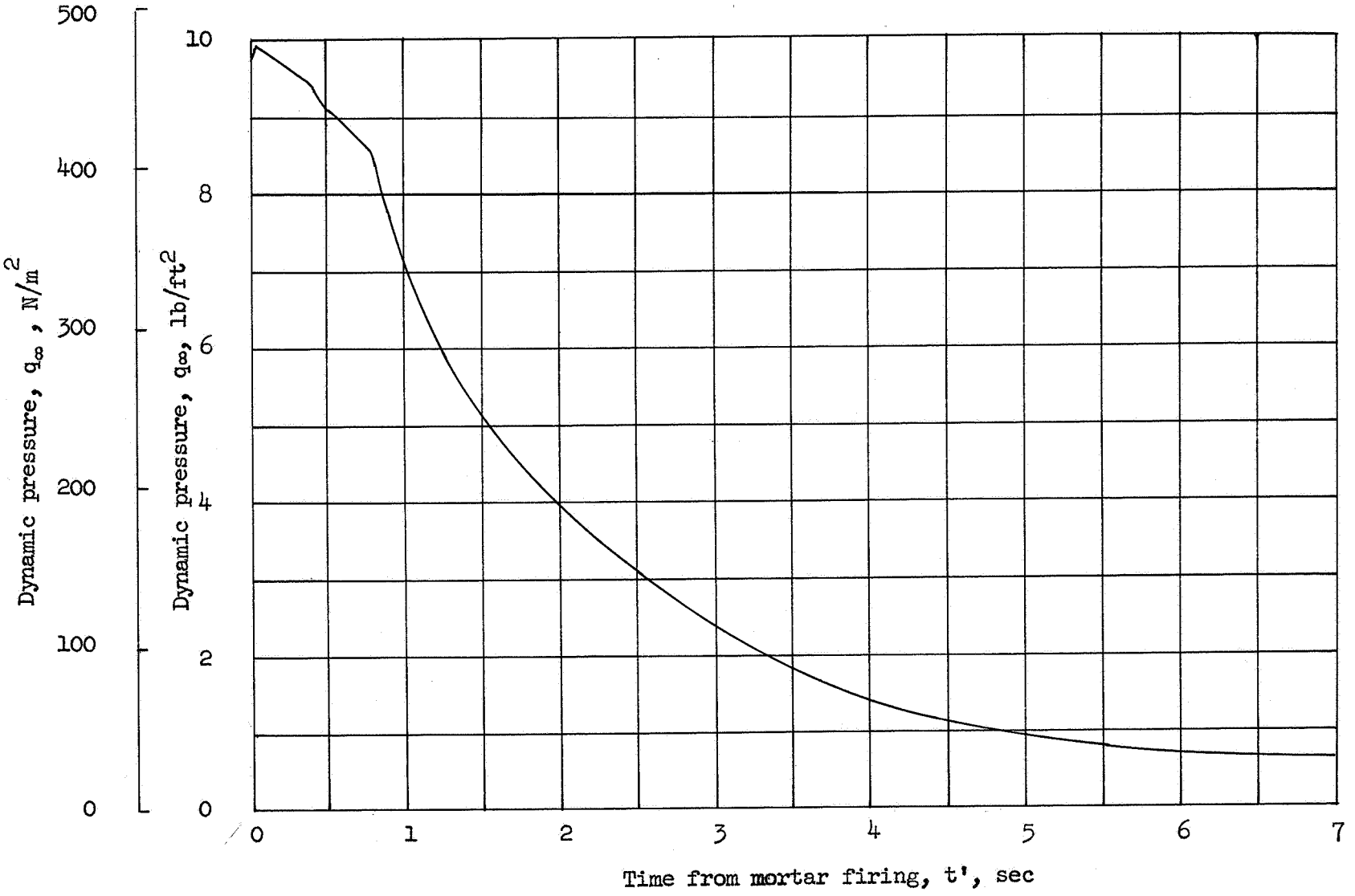

Figure 10.- Dynamic-pressure time history.

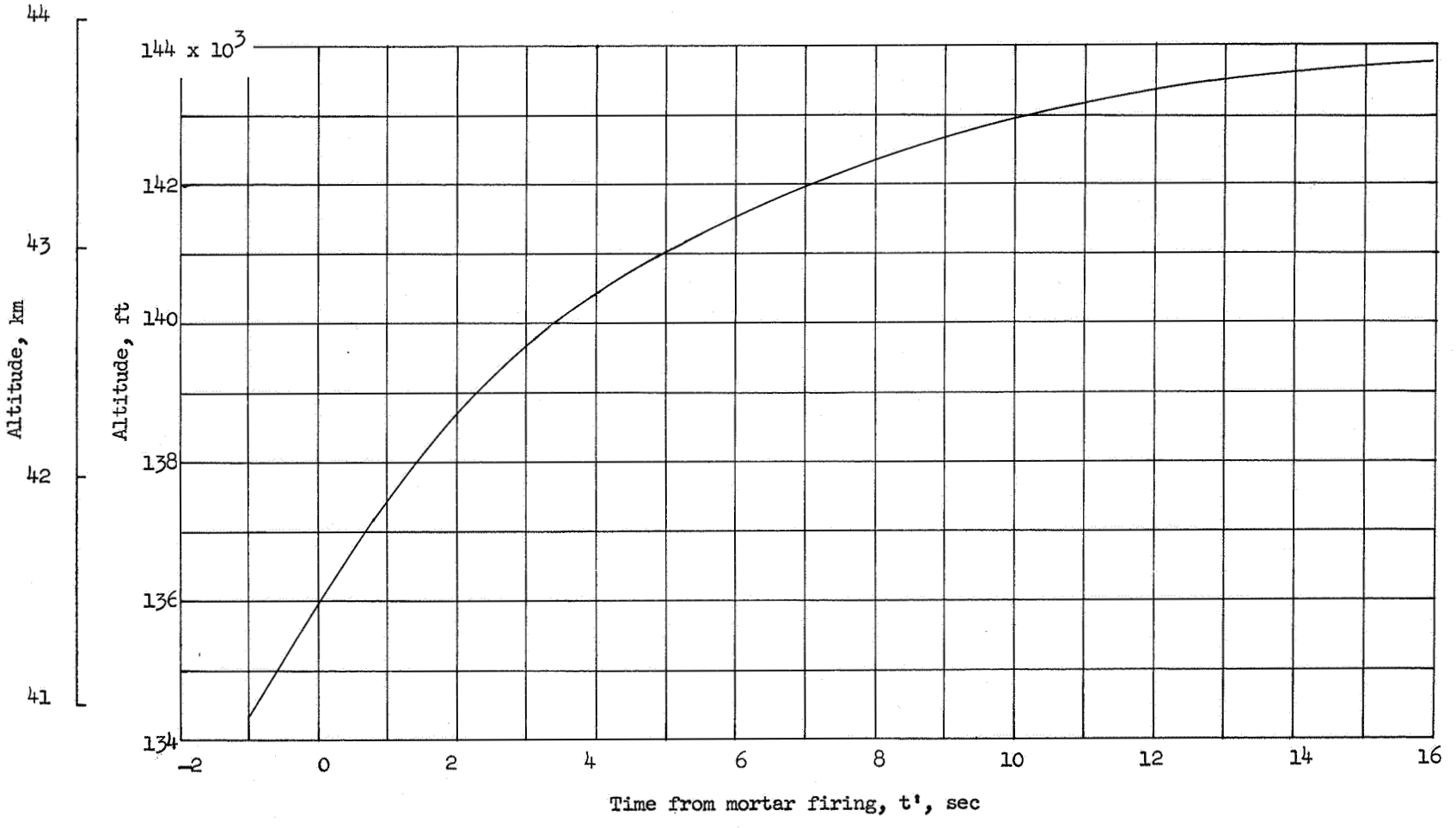

Figure 11.- Altitude time history.

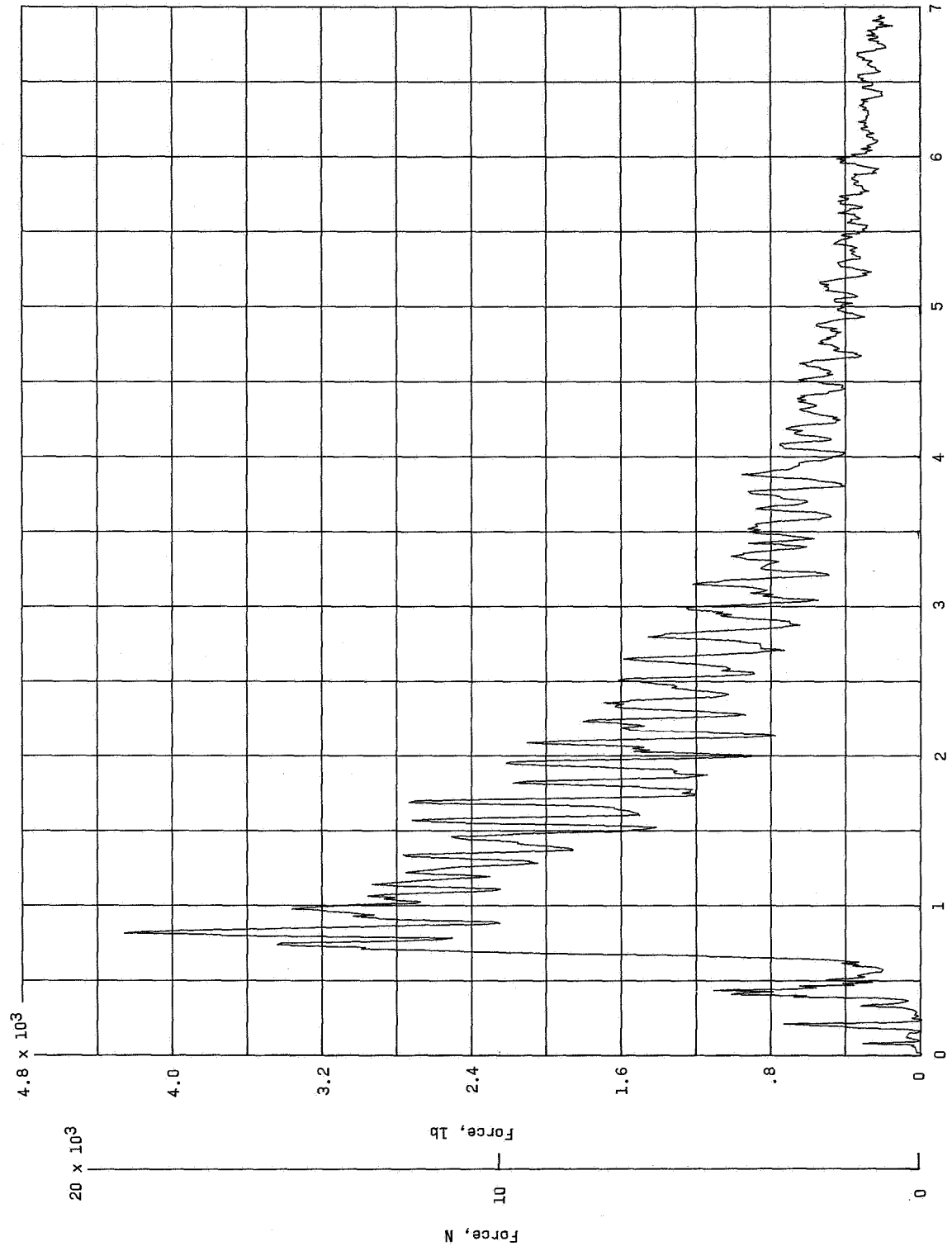

Figure 12.- Tensiometer-force time history.

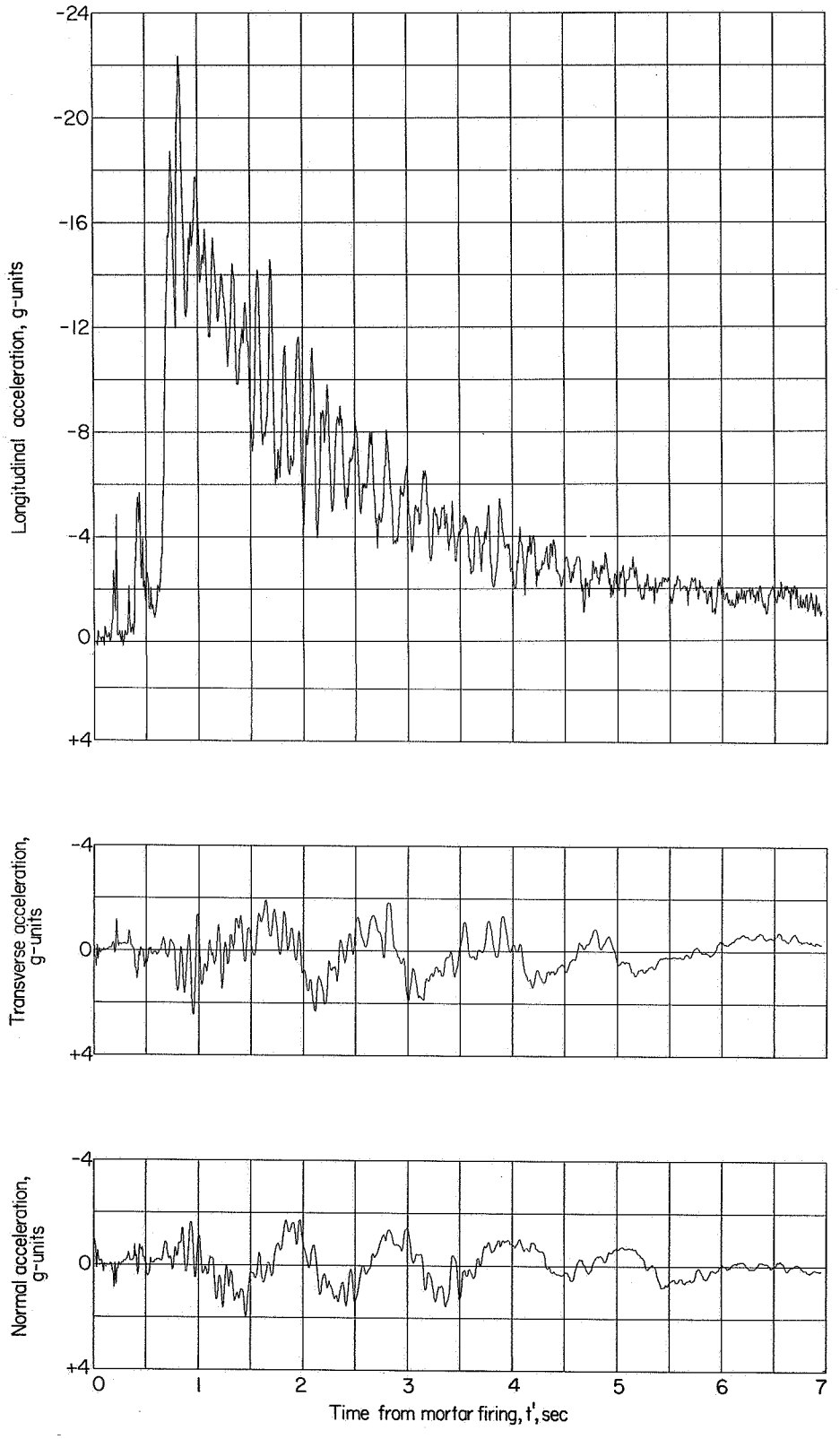

Figure 13.- Acceleration time histories.

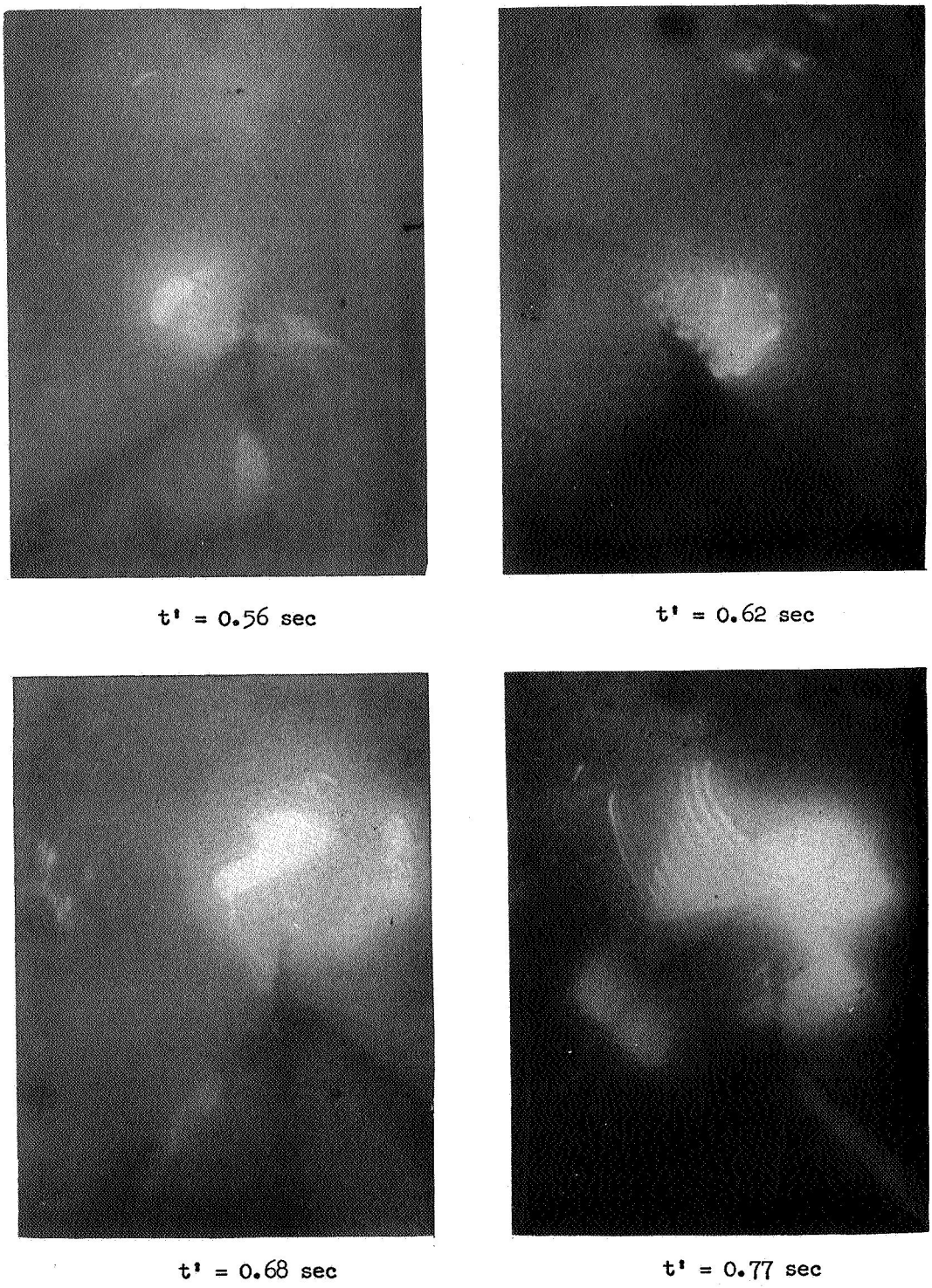

(a) Canopy inflation sequence. L-68-832

Figure 14.- Onboard camera photographs.

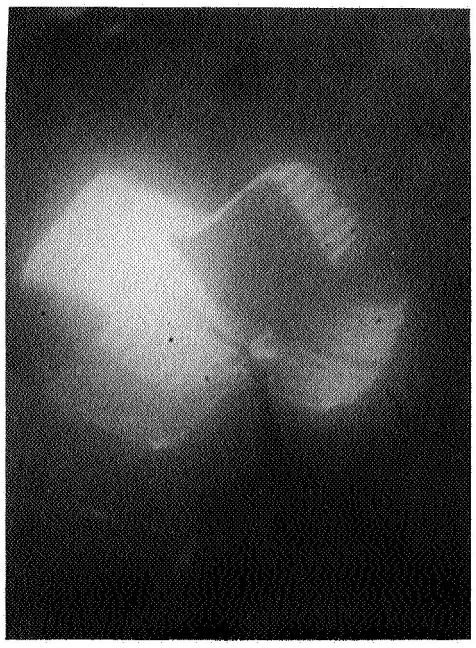

t' = 0.84 sec

t' = 0.87 sec

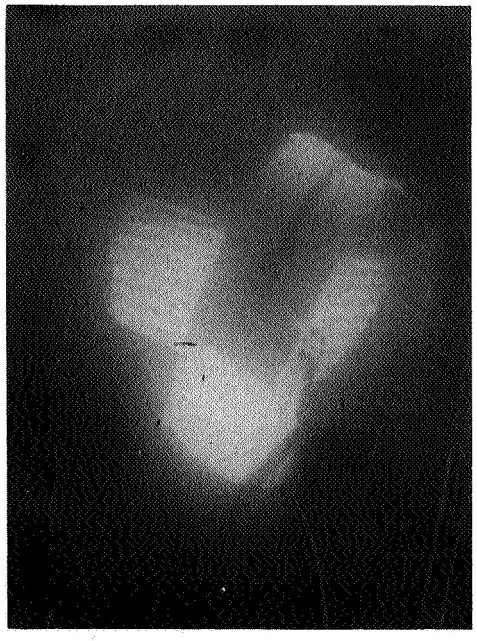

t' = 0.90 sec

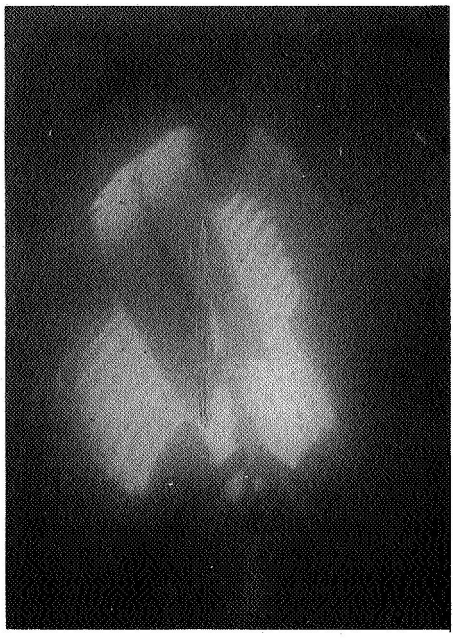

t' = 0.93 sec

(b) Canopy scissoring.

L-68-833

Figure 14.- Continued.

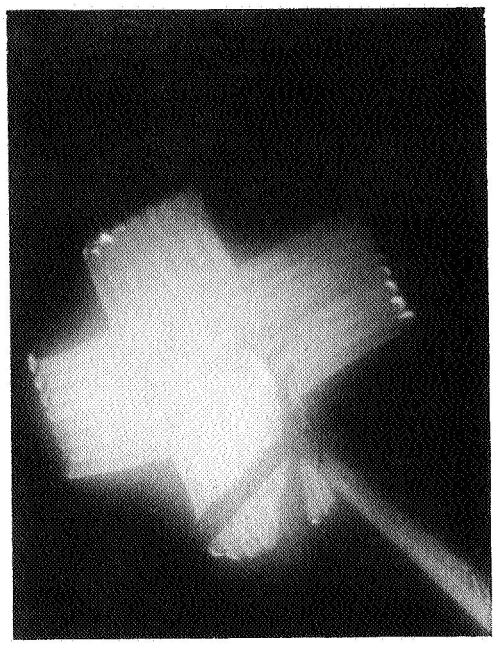

$t' = 34.00$ sec

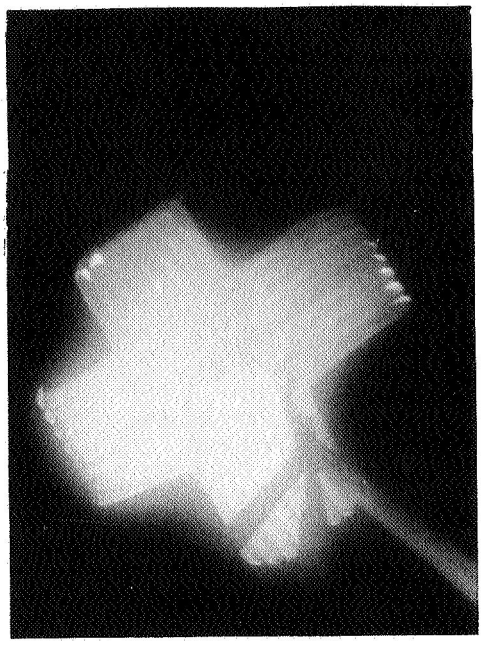

$t' = 34.03$ sec

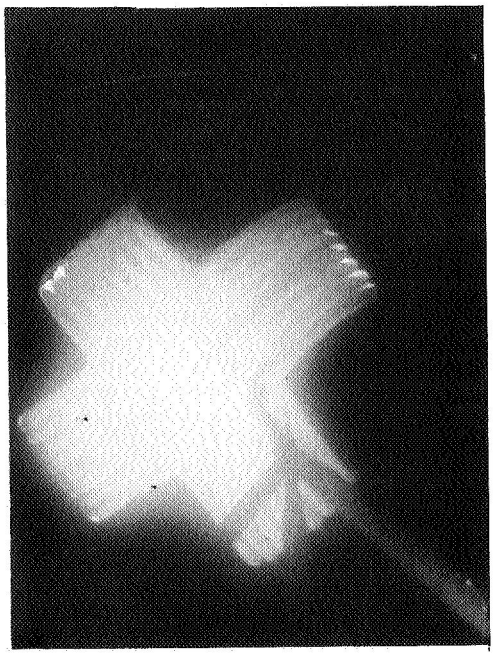

$t' = 34.06$ sec

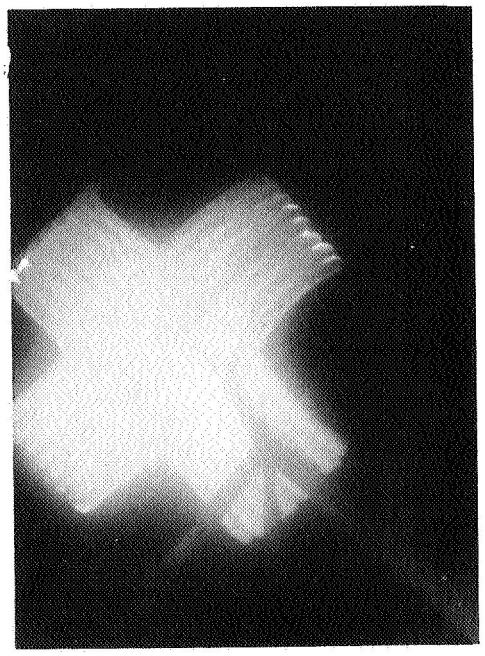

$t' = 34.09$ sec

(c) Parachute during descent.

L-68-834

Figure 14.- Concluded.

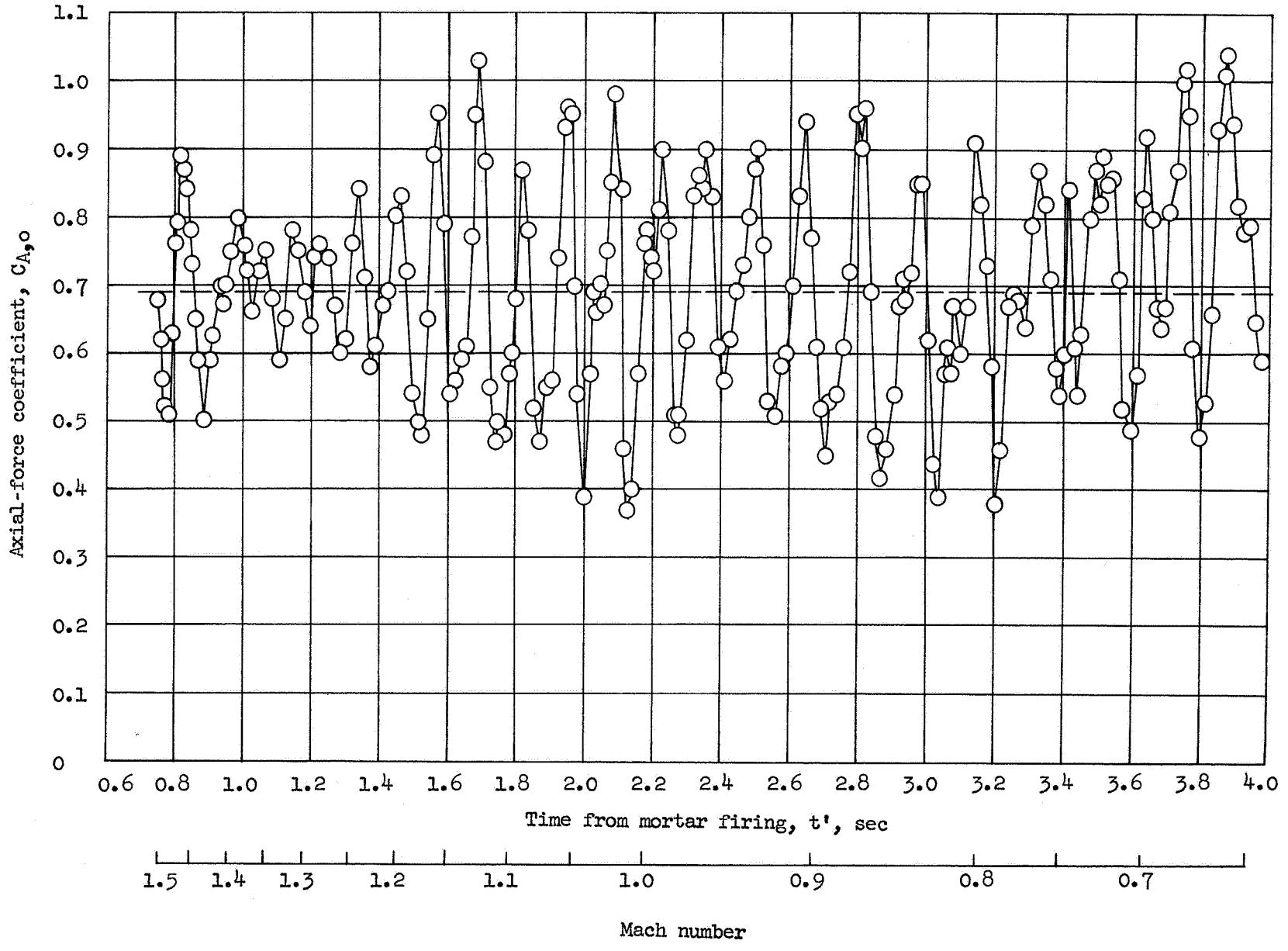

Figure 15.- Variation of axial-force coefficient with time and Mach number.

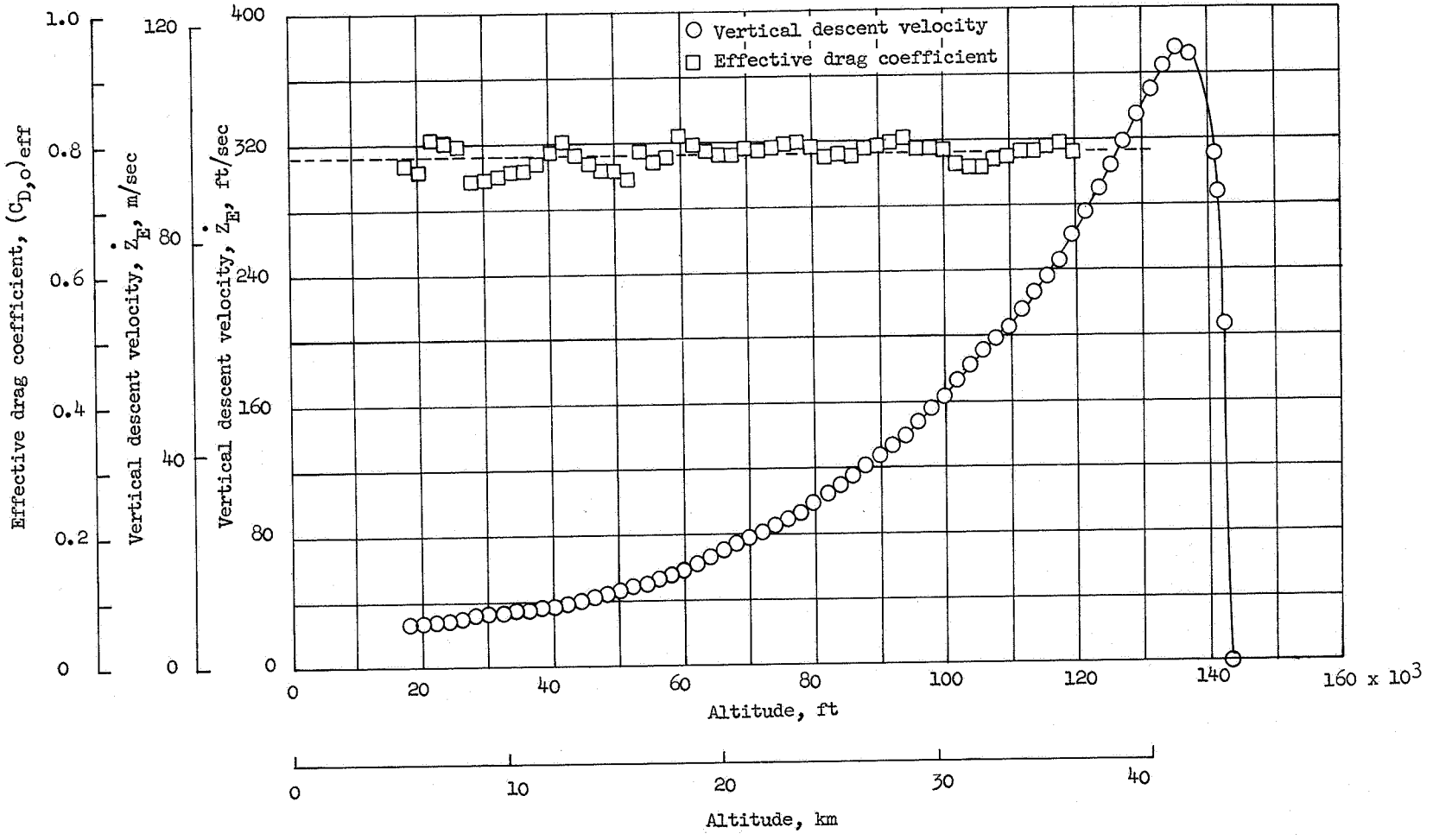

Figure 16.- Variation of vertical descent velocity and effective drag coefficient with altitude.

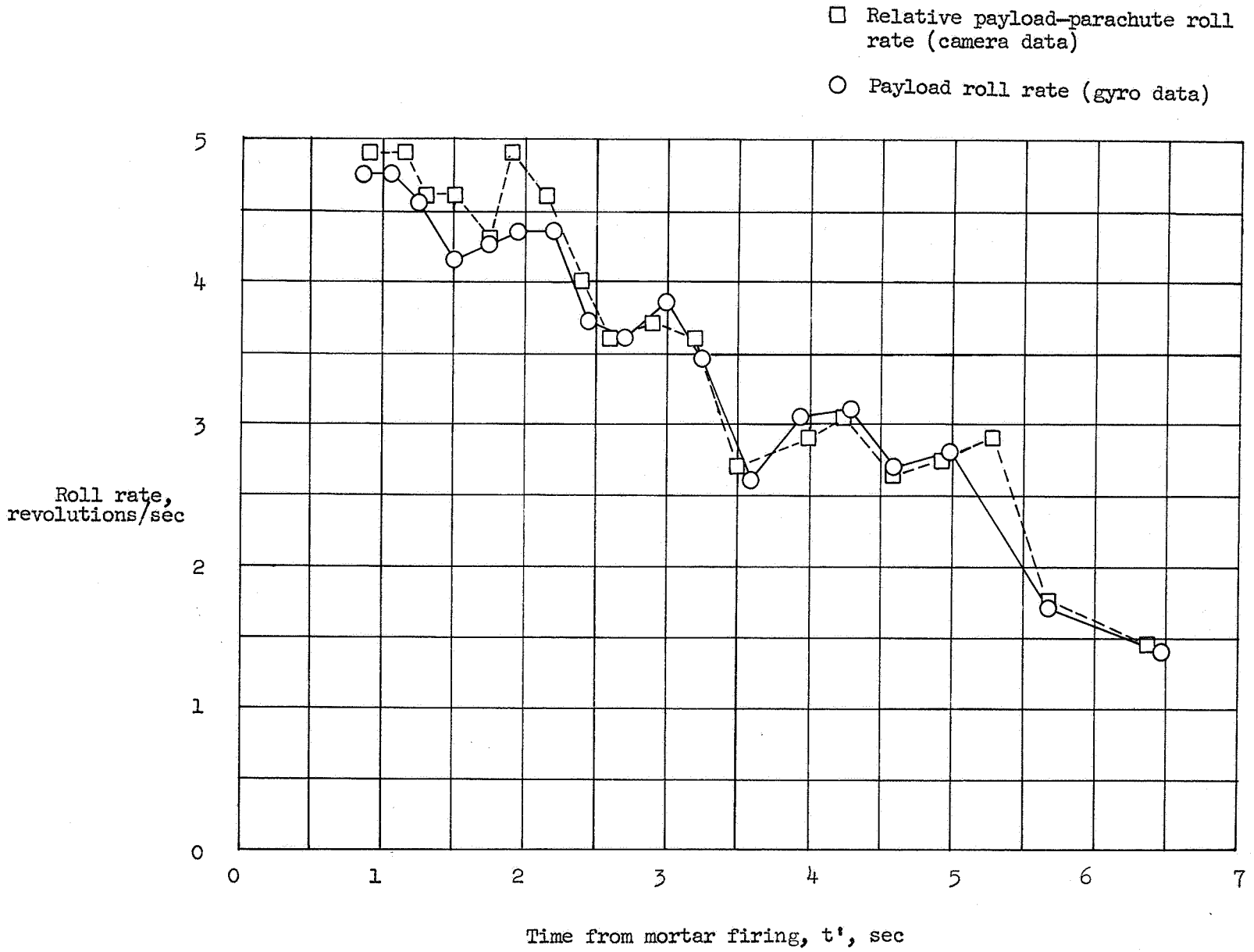

Figure 17.- Comparison of payload roll rate with relative payload-parachute roll rate.

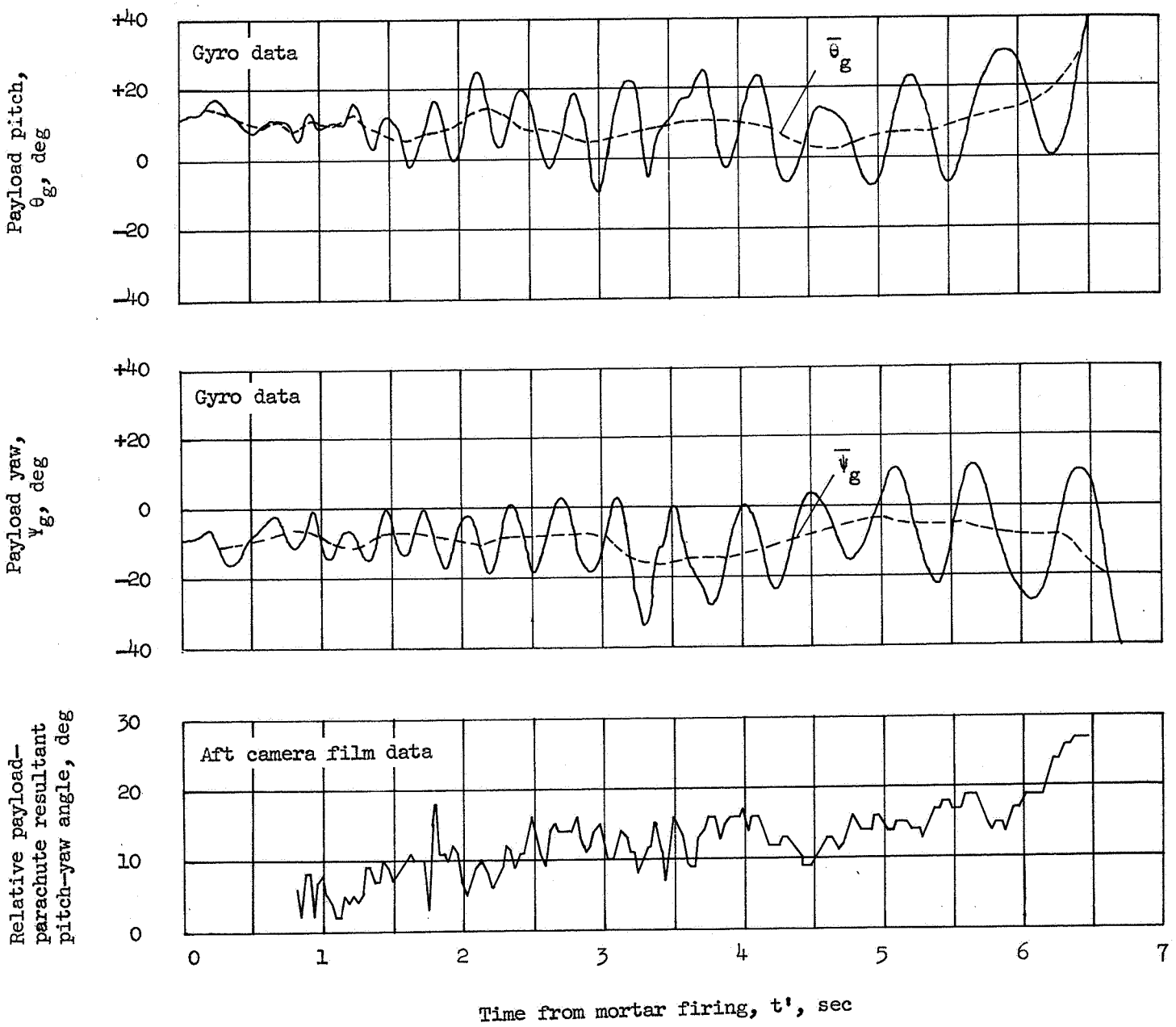

Figure 18.- Comparison of payload pitch and yaw with relative payload-parachute resultant pitch-yaw angle.

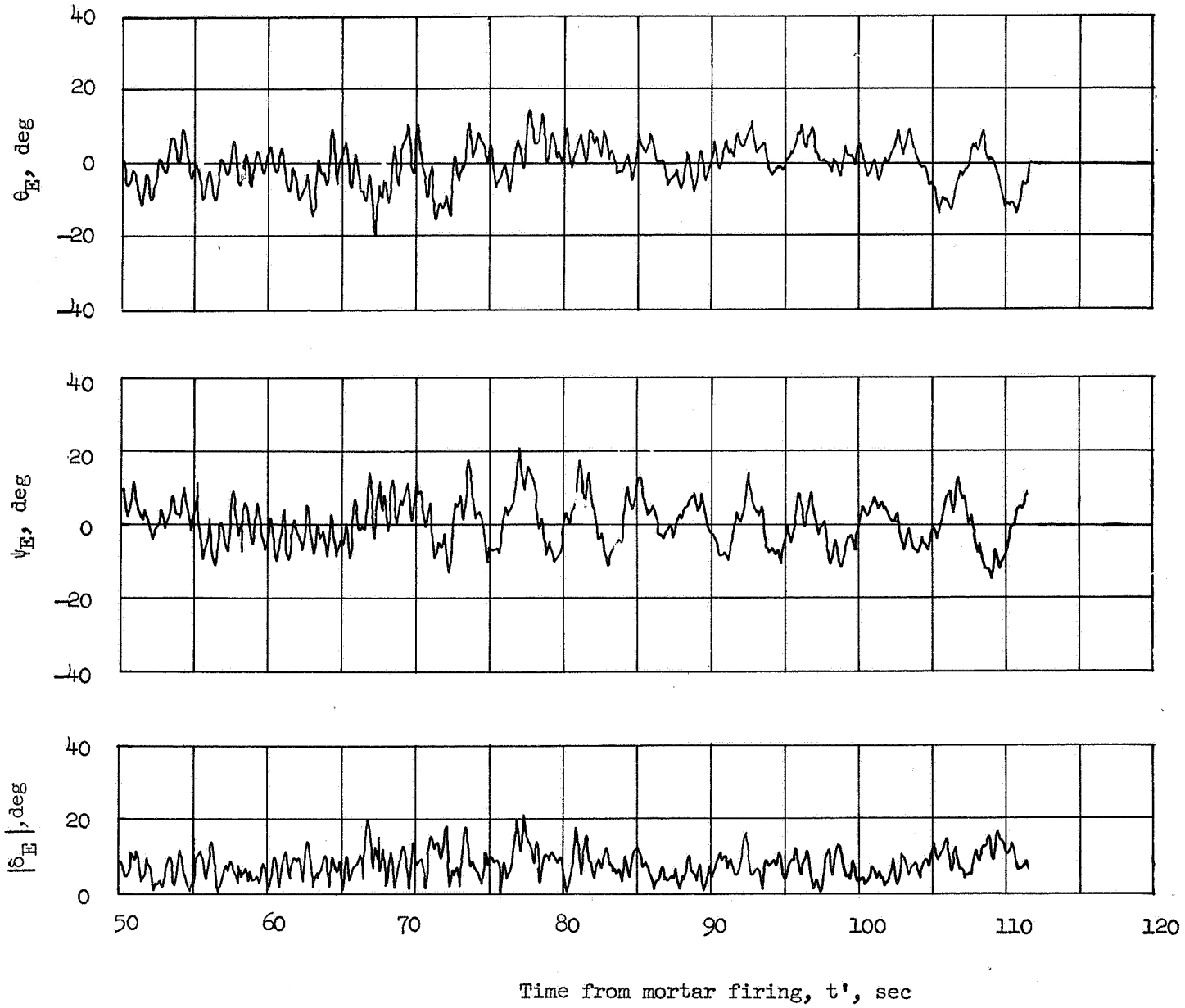

Figure 19.- Time histories of pitch θ_E, yaw ψ_E, and the magnitude of the resultant angular displacement $|\delta_E|$ of the payload from the local vertical for a portion of descent from 134 000 to 116 000 feet.

Figure 20.- Photograph of payload and parachute at recovery site.

L-68-835

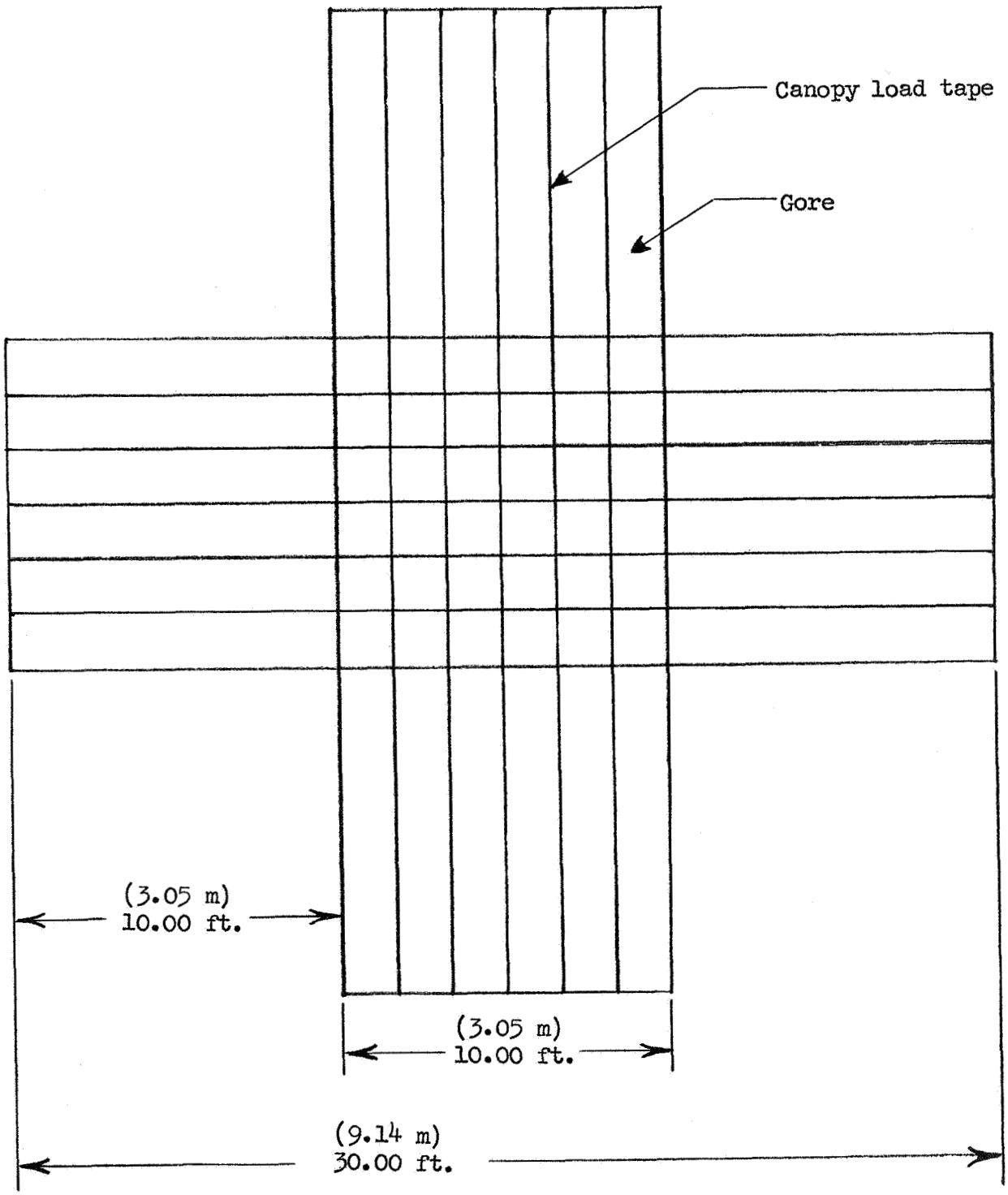

Figure 21.- Canopy layout of 0.333 width-length ratio cross parachute.

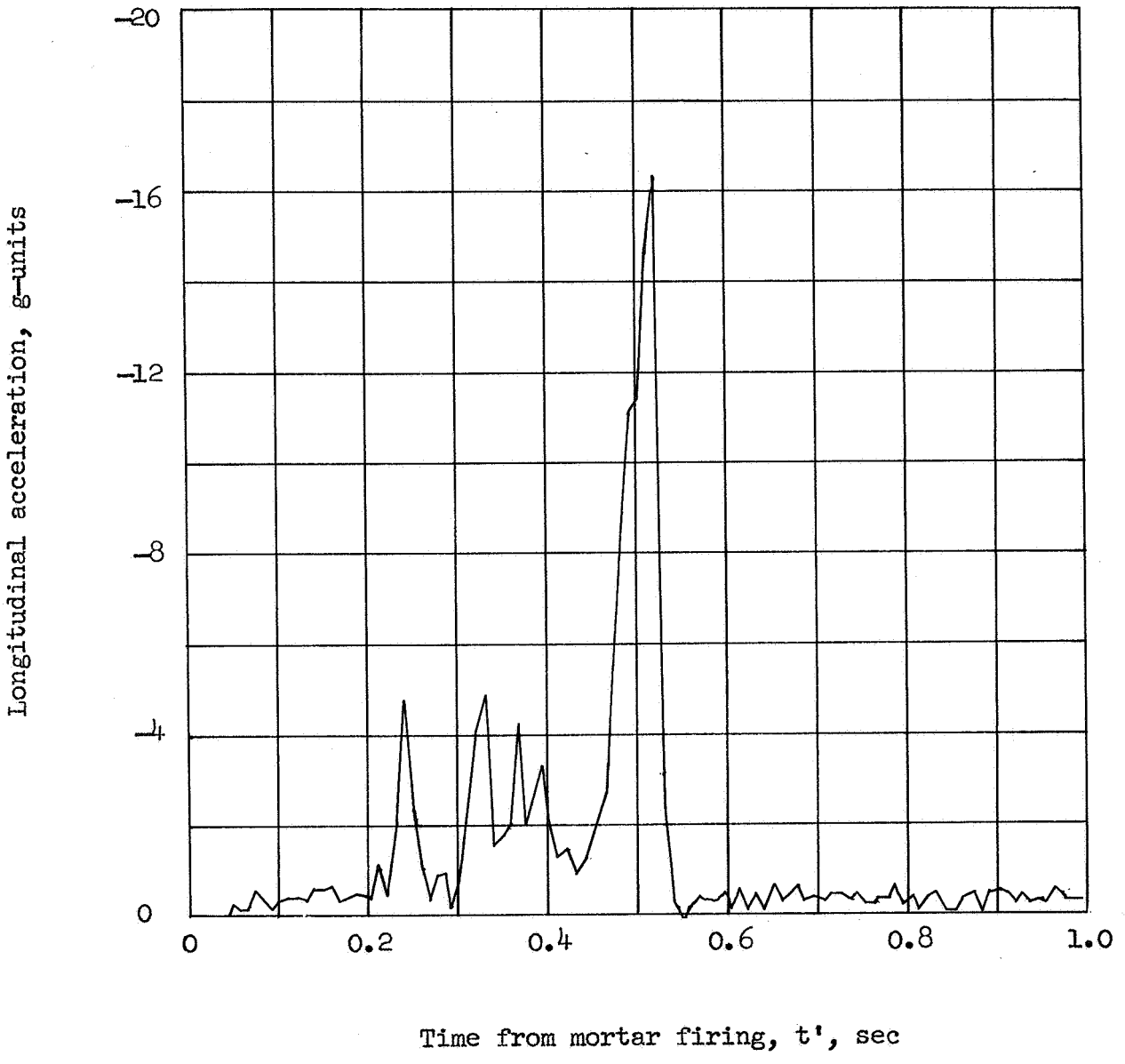

Figure 22.- Time history of longitudinal acceleration during deployment.

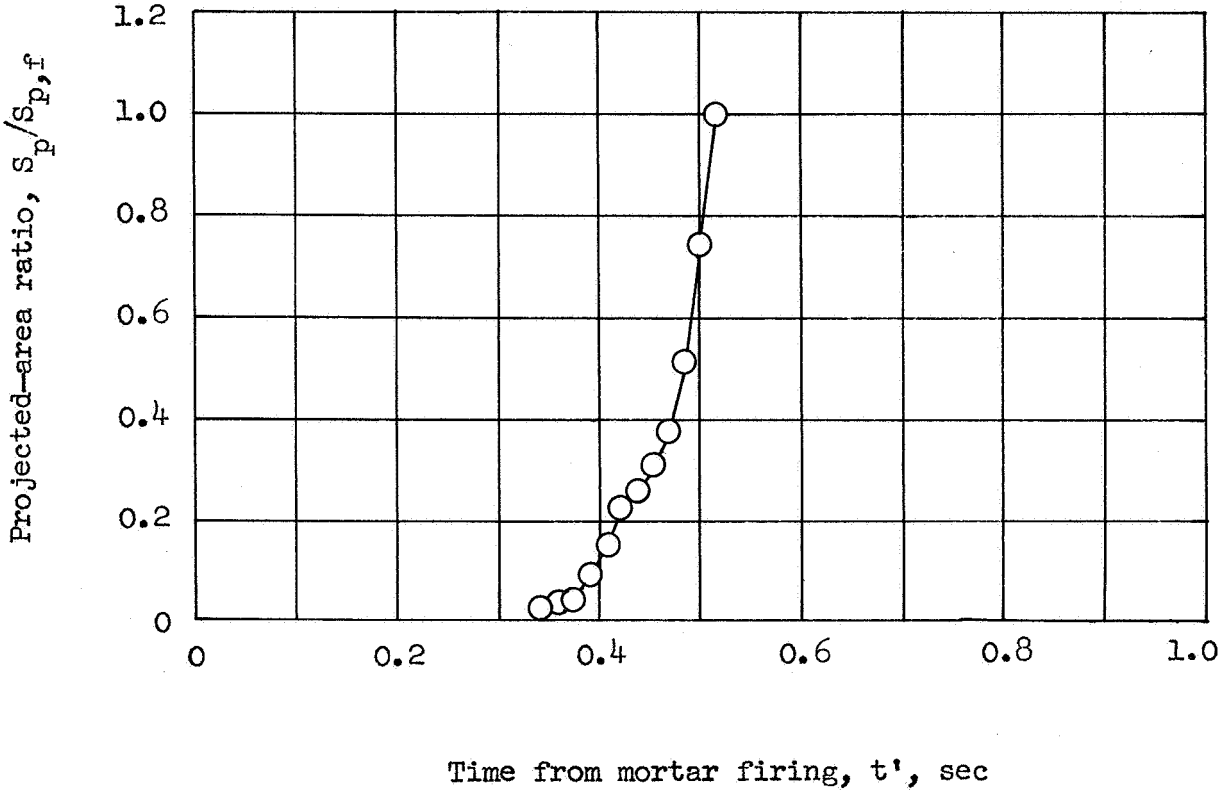

Figure 23.- Parachute projected-area-ratio time history.

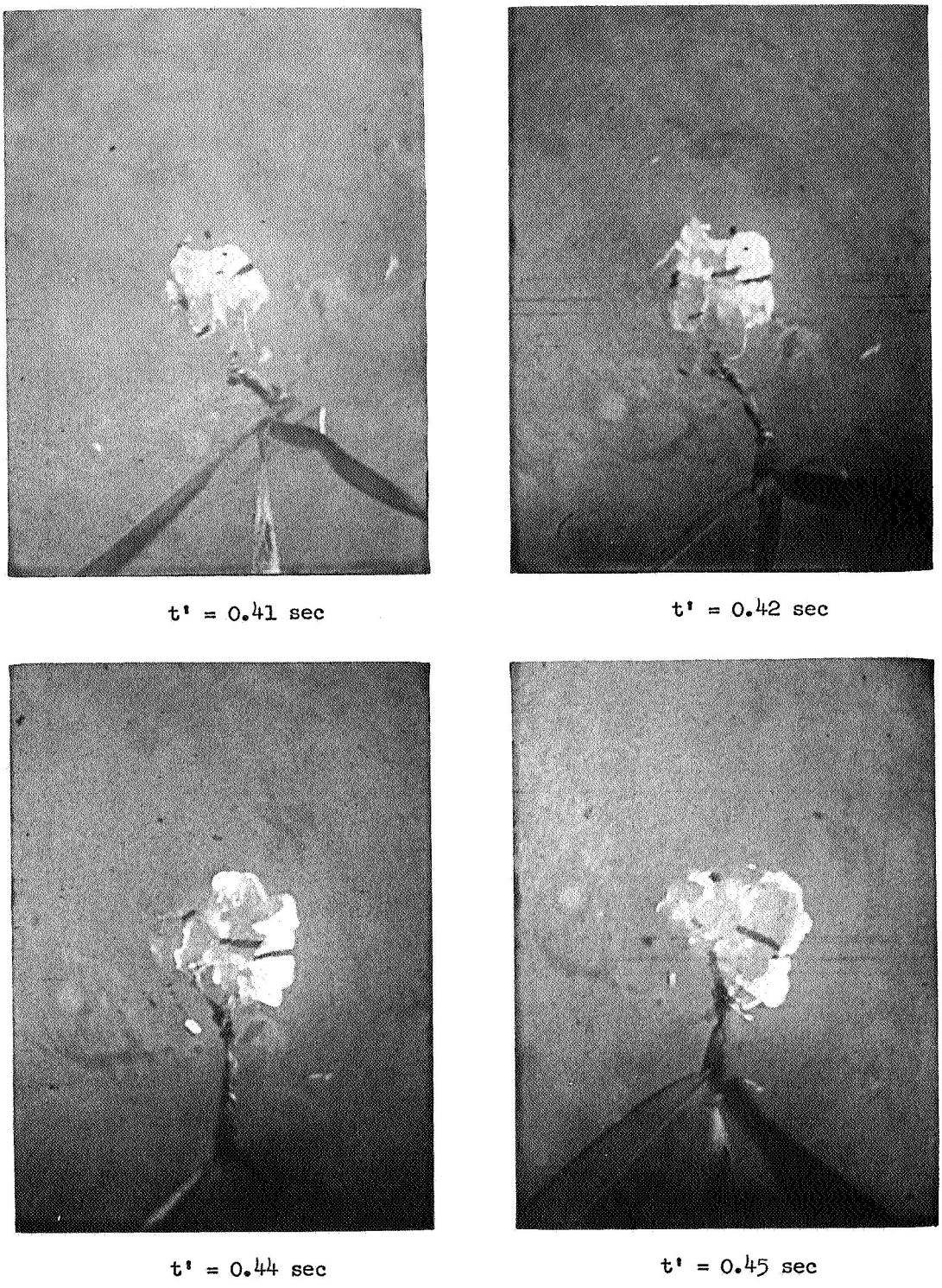

(a) Canopy inflation sequence.

L-68-836

Figure 24.- Onboard camera photographs.

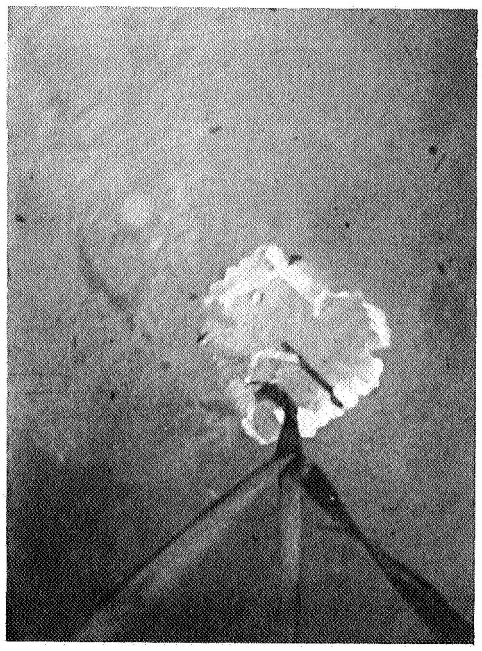

$t' = 0.47$ sec

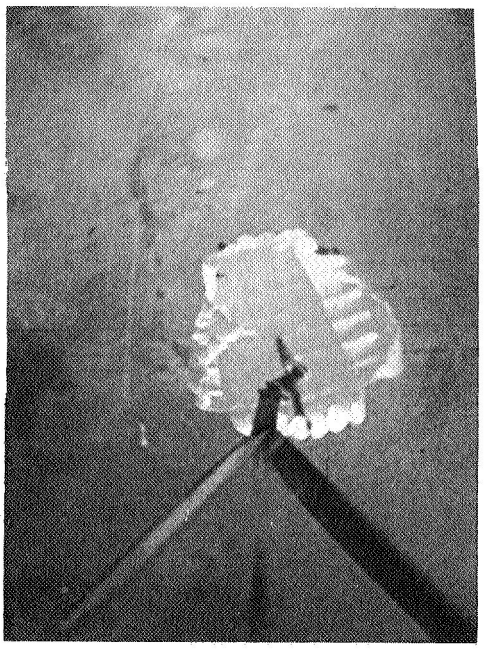

$t' = 0.49$ sec

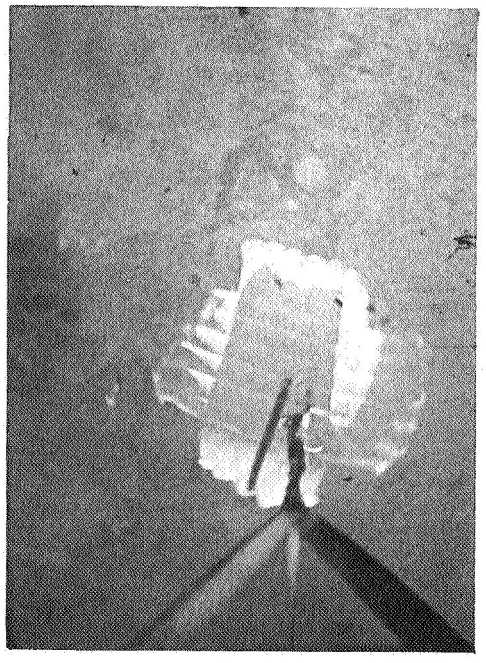

$t' = 0.50$ sec

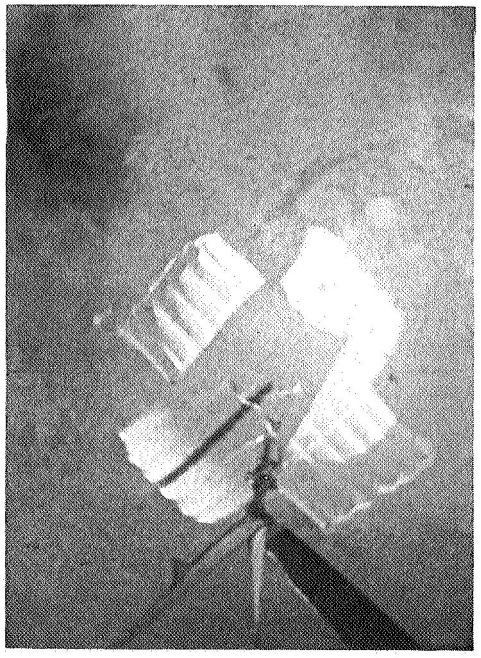

$t' = 0.51$ sec

(a) Concluded.

L-68-837

Figure 24.- Continued.

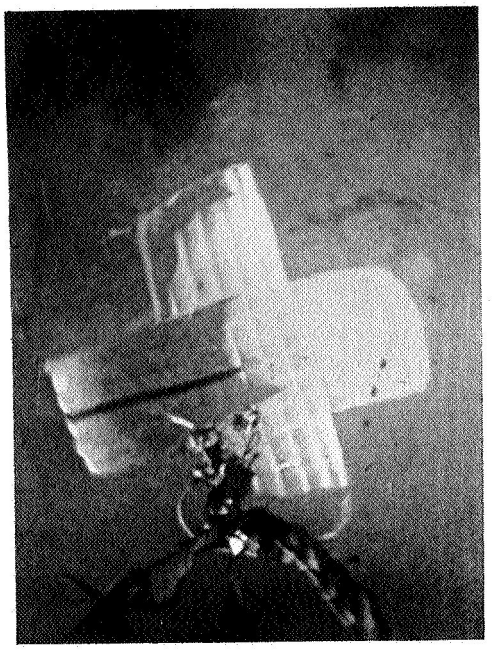

$t' = 0.53$ sec

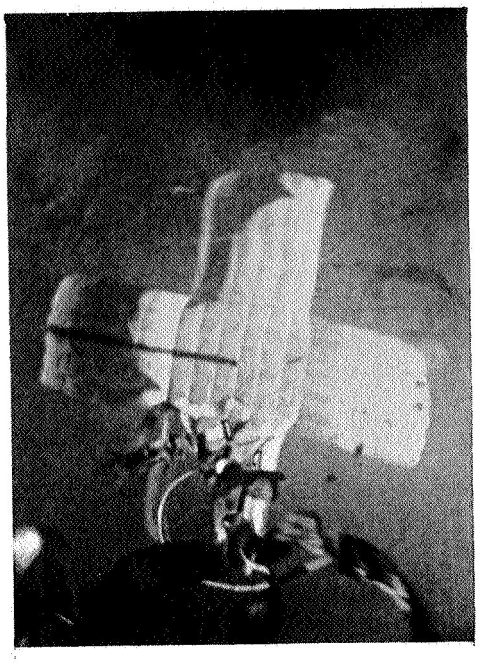

$t' = 0.55$ sec

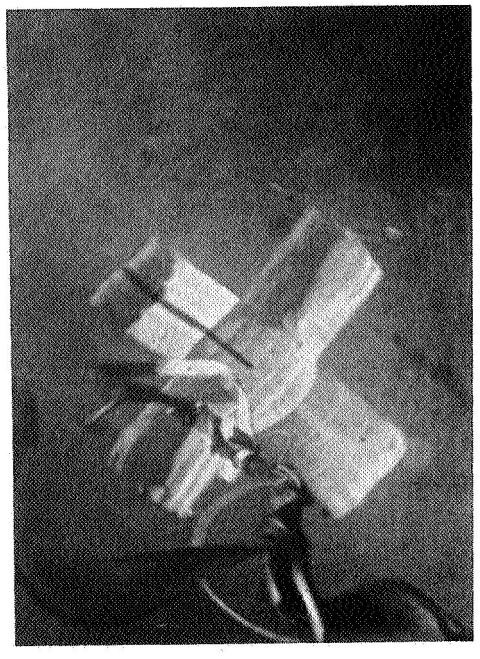

$t' = 0.56$ sec

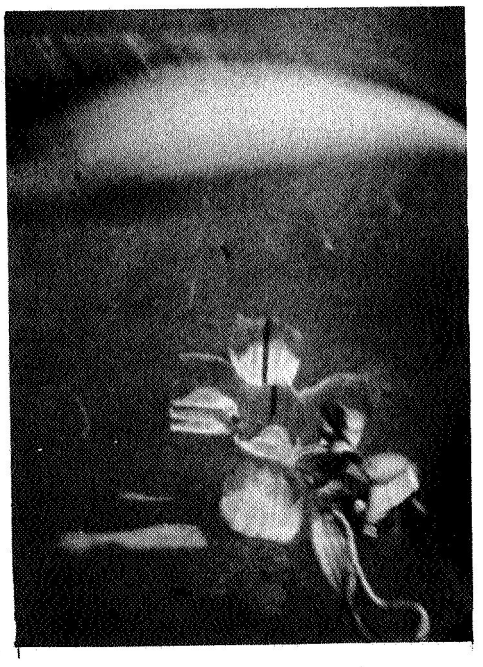

$t' = 0.59$ sec

(b) Parachute after separation from payload.

L-68-838

Figure 24.- Concluded.

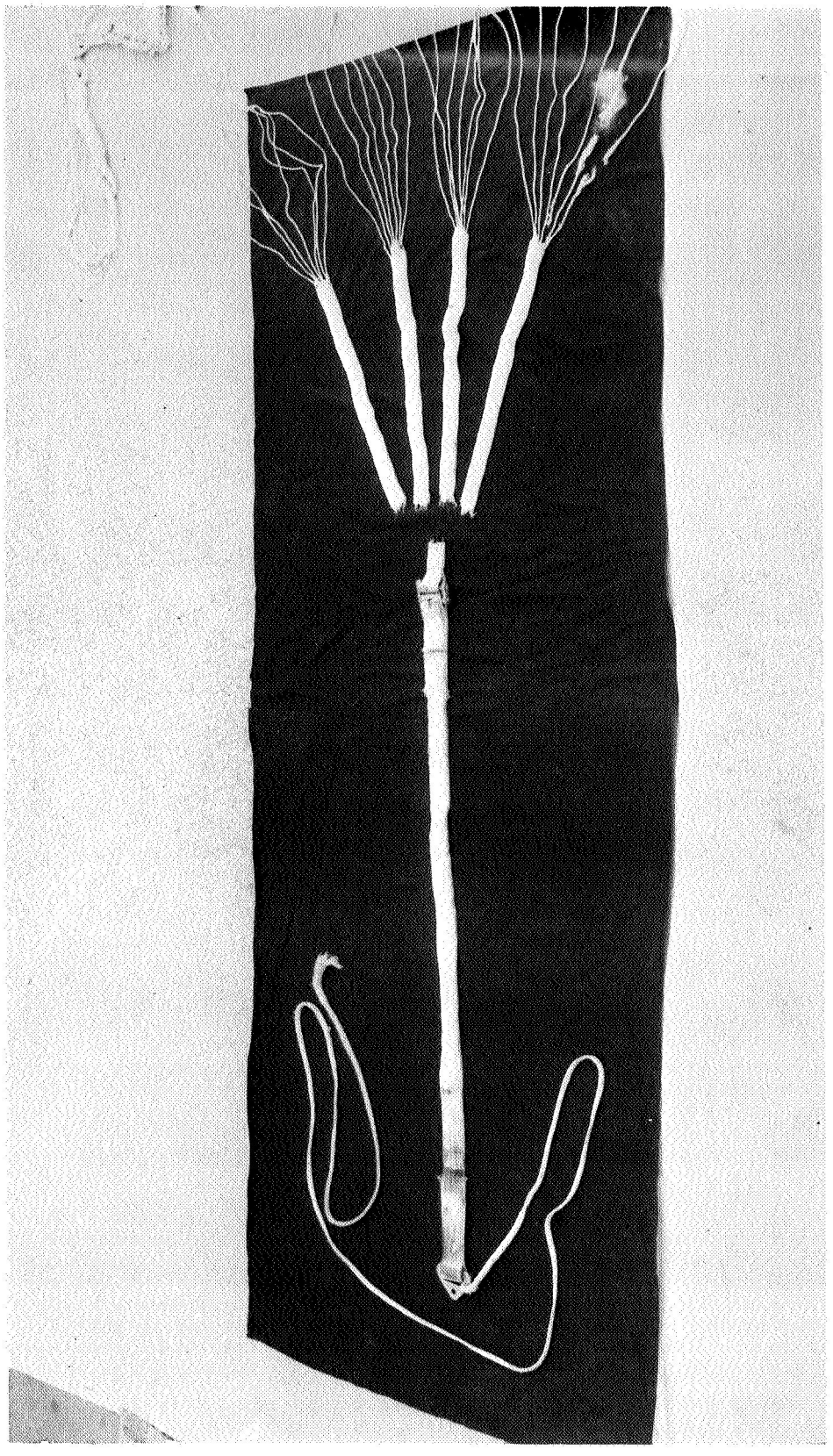

L-67-4012

Figure 25.- Closeup photograph of broken suspension-line attachment webbings.

A motion-picture film supplement L-994 is available on loan. Requests will be filled in the order received. You will be notified of the approximate date scheduled.

The film (16 mm, 3 min, color, silent) was taken by an onboard camera and shows deployment, inflation, and overall flight performance during the test of the 0.264 width-length ratio parachute.

Requests for the film should be addressed to:

Chief, Photographic Division
NASA Langley Research Center
Langley Station
Hampton, Va. 23365

CUT

Date_____

Please send, on loan, copy of film supplement L-994 to TM X-1542

_____

Name of organization

_____

Street number

_____

City and State Zip code

Attention: Mr._____

Title_____

Place
Stamp
Here

Chief, Photographic Division
NASA Langley Research Center
Langley Station
Hampton, Va. 23365